PERFORMANCE EVALUATION OF TECHNIQUES FOR TIME DELAY ESTIMATION

by

KENT N. SCARBROUGH

B.S., Kansas State University, 1976

A MASTER'S REPORT

submitted in partial fulfillment of the

requirements for the degree

MASTER OF SCIENCE

Department of Electrical Engineering

KANSAS STATE UNIVERSITY

Manhattan, Kansas

1980

Approved by:

Nasir Ahmed

Major Professor

TABLE OF CONTENTS

LIST OF FIGURES

LIST OF TABLES

CHAPTER I

INTRODUCTION

The problem of estimating the time delay between noisy signals received at two or more spatially separated sensors has attracted considerable interest in recent years. One important application is in the localization of an underwater acoustic source. If the source signal is received at atleast three remote sensors it is possible to estimate the range, as well as the bearing to the source, from the time delay estimate [1].

Many methods have been proposed to estimate the time delay parameter. Some of the related schemes are: (i) the Roth processor [2], (ii) the smoothed coherence transform (SCOT) [3], (iii) the phase transform (PHAT) [4], and (iv) the Eckart processor [5]. Also a maximum likelihood (ML) estimator has been derived [6] and it has been shown that the ML estimator is identical to that proposed by Hannan and Thompson [7]. The preceding methods have been shown to be related through a generalized cross correlation approach [6], and an expression for the variance of the time delay estimate for the generalized cross correlator has been derived [8].

The main objective of this work is to evaluate the performance of the SCOT algorithm and an approximate maximum likelihood estimator, as compared to the basic cross correlation method of estimating the time delay, via a digital simulation. The particular case considered is that of a narrow band random signal corrupted by white Gaussian noise received at three remote sensors. Using the time delay estimates obtained from the simulation, estimates of the range of the source are computed. The variances of the time delay estimates and the range estimates are then compared with the corresponding theoretical values.

A brief review of the theoretical aspects of this problem is presented in Chapter 2. Details of the simulation and the simulation results are given in Chapter 3. Then in Chapter 4, the implications of the results are discussed and conclusions are drawn.

CHAPTER II

SOME THEORETICAL CONSIDERATIONS

A simple but useful model of the two sensor problem is as follows:

$$\begin{aligned} x_1(t) &= s_1(t) + n_1(t) \\ x_2(t) &= s_1(t+D) + n_2(t) \end{aligned} \tag{2-1}$$

where $x_1(t)$ and $x_2(t)$ denote the sensor outputs, $s_1(t)$ is the source signal, and $n_1(t)$ and $n_2(t)$ represent the additive noise sources. It is assumed that $s(t)$, $n_1(t)$ and $n_2(t)$ are uncorrelated and jointly stationary real processes. The problem is then to estimate the time delay parameter D.

A common method of determining the delay is to compute the cross correlation function

$$R_{x_1x_2}(\tau) = E\,[x_1(t)\; x_2(t-\tau)] \tag{2-2}$$

where E is the expectation operator. The parameter τ that maximizes $R_{x_1x_2}(\tau)$ in (2-2) is an estimate of the time delay D. The cross correlation can be computed from the cross power spectral density function using the Fourier Transform relationship

$$R_{x_1x_2}(\tau) = \int_{-\infty}^{\infty} G_{x_1x_2}(f)\; e^{j2\pi f\tau}\; df. \tag{2-3}$$

However, in practice only an estimate, say $\hat{G}_{x_1x_2}(f)$, of $G_{x_1x_2}(f)$ can be obtained due to the finite observation interval. Thus only an estimate, $\hat{R}_{x_1x_2}(\tau)$, of the cross correlation function can be computed.

In an effort to reduce the error in the time delay estimate induced by the spectral estimation, several other methods have been developed. It has been shown by Knapp and Carter [6] that many of these methods, in particular those noted in the introduction, can be related by a generalized cross correlation method. In this approach the sensor outputs $x_1(t)$ and $x_2(t)$

are pre-filtered as depicted in Fig. 2.1. The cross power spectrum between the filter outputs $y_1(t)$ and $y_2(t)$ can then be computed [9] as

$$G_{y_1y_2}(f) = H_1(f)\, H_2^*(f)\, G_{x_1x_2}(f) \tag{2-4}$$

where * denotes the complex conjugate. The generalized cross correlation function is then given by

$$R_{y_1y_2}(\tau) = \int_{-\infty}^{\infty} W(f)\, G_{x_1x_2}(f)\, e^{j2\pi f\tau}\, df \tag{2-5}$$

where $W(f) = H_1(f)\, H_2^*(f)$ is a weighting function.

Choosing $H_1(f) = H_2(f) = 1$, hence $W(f) = 1$ in (2-5) yields the basic cross correlation method. Other choices of W(f) yield the Roth processor, the SCOT algorithm, the phase transform, the Eckart processor, and the Hannan-Thompson or ML estimator as discussed in [6]. In this effort only the SCOT and the ML estimator will be considered, other than the basic cross correlation method.

The motivation behind the SCOT algorithm is the desire to counteract errors in the estimate of $G_{x_1x_2}(f)$ caused by frequency bands where the noise power, either $G_{n_1n_1}(f)$ or $G_{n_2n_2}(f)$ is large. The weighting function is therefore chosen to be

$$W(f) = \frac{1}{\left[G_{x_1x_1}(f)\, G_{x_2x_2}(f)\right]^{1/2}} \tag{2-6}$$

where

$$G_{x_ix_i}(f) = G_{s_1s_1}(f) + G_{n_in_i}(f)\ ;\ i = 1,2. \tag{2-7}$$

Substituting this weight function in (2-5) and noting that in most cases the auto spectra $G_{x_1x_1}(f)$ and $G_{x_2x_2}(f)$ must be estimated as well as the cross spectrum, one obtains

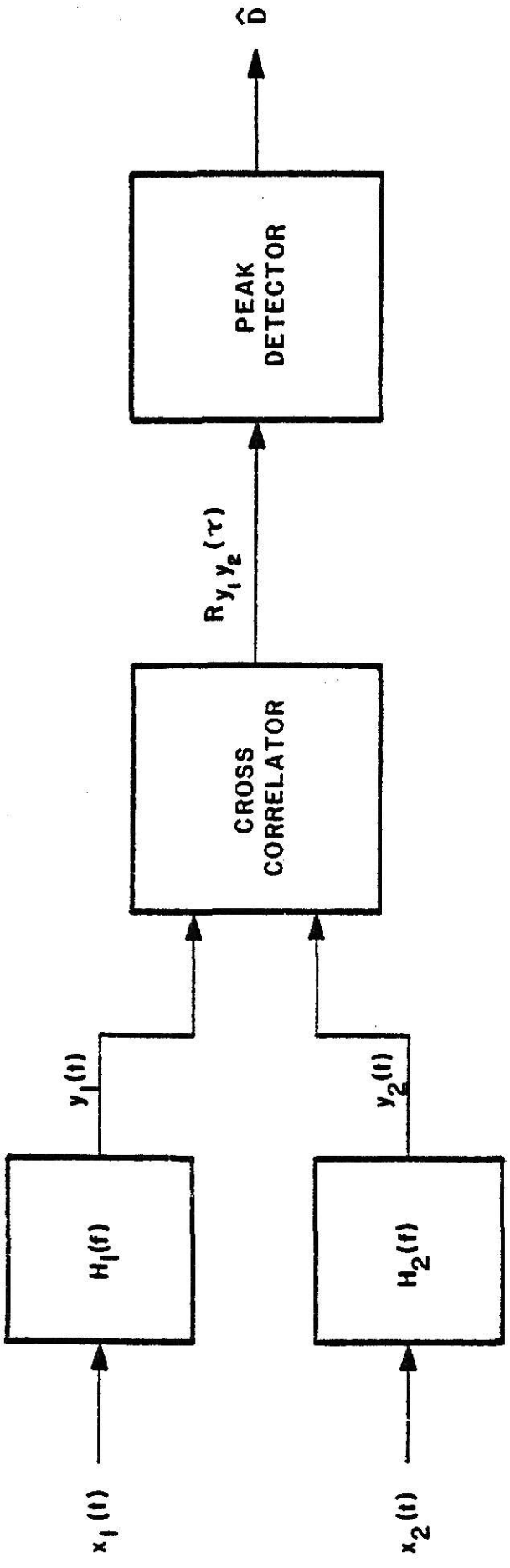

Fig. 2.1 Generalized Cross Correlation Method

$$\hat{R}_{y_1y_2}(\tau) = \int_{-\infty}^{\infty} \frac{\hat{G}_{x_1x_2}(f)e^{j2\pi f\tau}}{\sqrt{\hat{G}_{x_1x_1}(f)\,\hat{G}_{x_2x_2}(f)}}\ df. \qquad (2\text{-}8)$$

Returning to the realization of Fig. 2.1, if $H_1(f) = 1/\sqrt{G_{x_1x_1}(f)}$ and $H_2(f) = 1/\sqrt{G_{x_2x_2}(f)}$, the SCOT method can be interpreted as two pre-whitening filters which are followed by a cross correlator. Thus the effect of any dominant frequency components in $G_{x_1x_2}(f)$ is reduced when computing the inverse Fourier Transform. In fact the quantity

$$\gamma_{x_1x_2}(f) = \frac{G_{x_1x_2}(f)}{\sqrt{G_{x_1x_1}(f)\,G_{x_2x_2}(f)}} \qquad (2\text{-}9)$$

which is the complex coherence function between x_1 and x_2, has the property that $0 \le |\gamma_{x_1x_2}(f)| \le 1$. Further $|\gamma_{x_1x_2}(f)| = 0$ if x_1 and x_2 are uncorrelated and $|\gamma_{x_1x_2}(f)| = 1$ if x_1 and x_2 are linearly related. If the noises are uncorrelated $G_{n_1n_2}(f) = 0$, then

$$G_{x_1x_2}(f) = G_{s_1s_1}(f)\, e^{-j2\pi fD} \quad . \qquad (2\text{-}10)$$

Thus in frequency bands where the noise is dominant $|\gamma_{x_1x_2}(f)|$ is small and these bands are suppressed while frequency bands where the signal is dominant and $|\gamma_{x_1x_2}(f)|$ approaches 1 are emphasized. Finally it should be noted that the SCOT is obtained by taking the inverse Fourier Transform of $\gamma_{x_1x_2}(f)$; i.e.,

$$R_{y_1y_2}(\tau) = \int_{-\infty}^{\infty} \gamma_{x_1x_2}(f)\, e^{j2\pi f\tau}\ df. \qquad (2\text{-}11)$$

The maximum likelihood (ML) estimator is obtained by taking the weighting function to be

$$W(f) = \frac{C_{x_1x_2}(f)}{|G_{x_1x_2}(f)|\,[1 - C_{x_1x_2}(f)]} \tag{2-12}$$

where

$$C_{x_1x_2}(f) = |\gamma_{x_1x_2}(f)|^2 \tag{2-13}$$

is the magnitude squared coherence (MSC). Note that as long as $n_1(t)$ and $n_2(t)$ in (2-1) are not both zero processes, $C_{x_1x_2}(f) < 1$, and hence $W(f)$ in (2-12) is well defined. Again due to the necessity of estimating $G_{x_1x_2}(f)$ and $C_{x_1x_2}(f)$ in practice, it is not possible to achieve the ML estimator exactly. Substituting the corresponding estimate of $W(f)$ from (2-12) into (2-5) yields the approximate maximum likelihood (AML) estimator

$$\hat{R}_{y_1y_2}(\tau) = \int_{-\infty}^{\infty} \frac{\hat{C}_{x_1x_2}(f)\,\hat{G}_{x_1x_2}(f)\,e^{j2\pi f\tau}}{|\hat{G}_{x_1x_2}(f)|\,[1 - \hat{C}_{x_1x_2}(f)]}\,df. \tag{2-14}$$

Thus the time delay estimate, D, for the generalized cross correlator is given by the argument τ that maximizes $R_{y_1y_2}(\tau)$ in (2-5) where the cross spectrum $G_{x_1x_2}(f)$ and usually the weighting function $W(f)$ must be estimated from the data. An expression for the variance of the time delay estimates in the neighborhood of the true delay for any given weighting function is given by [8]

$$\sigma_D^2 = \frac{\int_{-\infty}^{\infty} |W(f)|^2\,(2\pi f)^2\,G_{x_1x_1}(f)\,G_{x_2x_2}(f)\,[1 - C_{x_1x_2}(f)]\,df}{T\left[\int_{-\infty}^{\infty} (2\pi f)^2\,|G_{x_1x_2}(f)|\,W(f)\,df\right]^2} \tag{2-15}$$

where T denotes the observation time in seconds.

To this point a two sensor model has been considered. The above results are easily extended to the three sensor model by first considering the time delay between sensor 1 and sensor 2, denoted by D_{21}, and then the time delay between sensors 2 and 3 denoted by D_{32}. Assuming that the sensors are collinear [see Fig. 2.2] and that the distance between sensors and the speed of sound is known, an estimate of the range can be computed from the time delay estimate. The range from the source to the central sensor is given by [10]

$$R = \frac{L_1 \left[1 - (CD_{21}/L_1)^2\right] + L_2 \left[1 - (CD_{32}/L_2)^2\right]}{2 \left[CD_{32}/L_2 - CD_{21}/L_1\right]} \tag{2-16}$$

where

L_1 = distance between sensors 1 and 2,

L_2 = distance between sensors 2 and 3,

C = speed of sound,

and $D_{ij} = D_i - D_j$ = the time delay between sensors i and j for i,j = 1,2,3. Also it has been shown that the variance of the error of the range estimate is given by [10]

$$\sigma^2_{\Delta R} \simeq 2\left(\frac{R}{L_e}\right)^4 C^2 \quad \sigma^2_{\Delta D_{31}} \tag{2-17}$$

where L_e is the effective half array length, and $\sigma^2_{\Delta D_{31}}$ is the variance of the error in estimating the time delay from sensor 3 to 1.

In the next chapter the results of a digital simulation are presented comparing the SCOT algorithm and the AML estimator with the basic cross correlation method of estimating the time delay and the range of the source. The variances of these experimental results are then compared with the theoretical values obtained via (2-15) and(2-17).

THIS BOOK CONTAINS NUMEROUS PAGES WITH DIAGRAMS THAT ARE CROOKED COMPARED TO THE REST OF THE INFORMATION ON THE PAGE.

THIS IS AS RECEIVED FROM CUSTOMER.

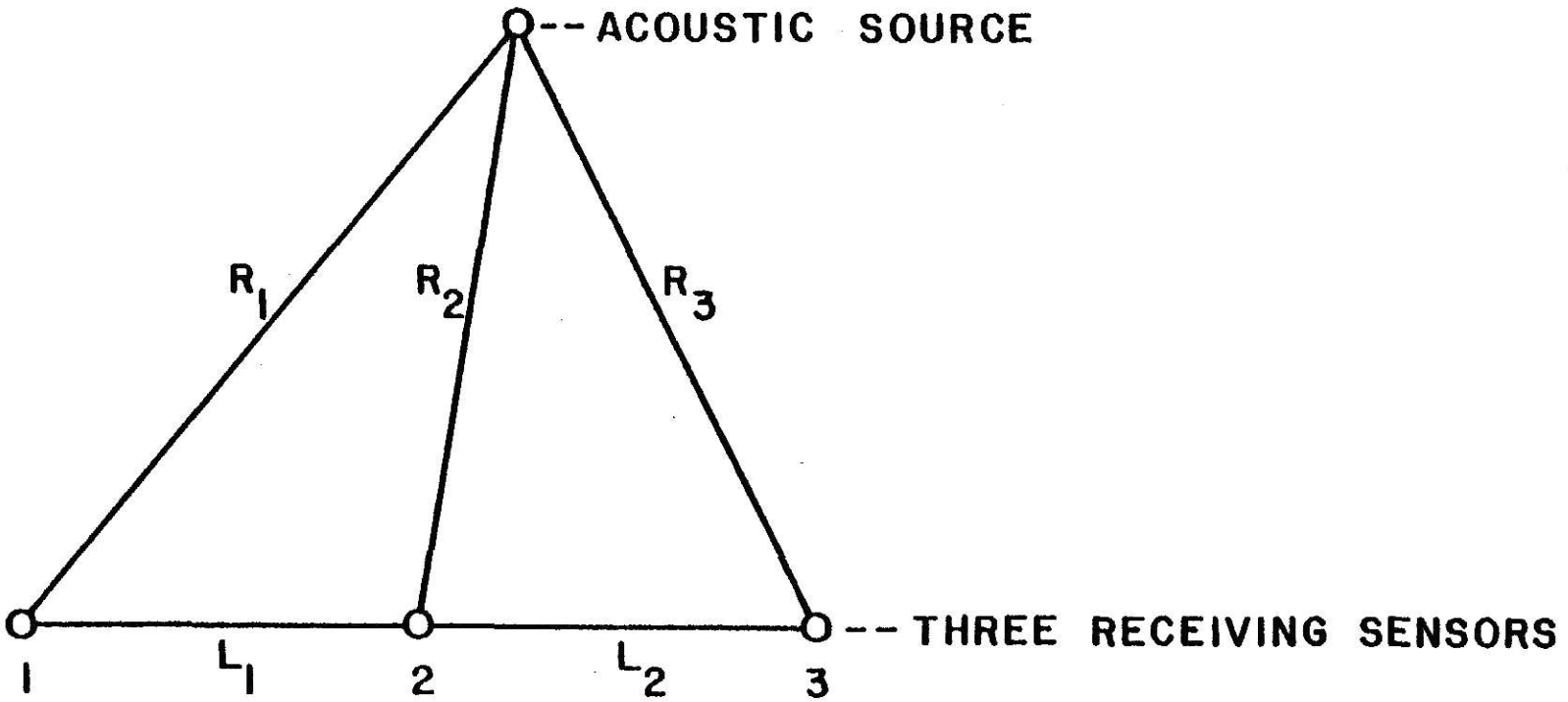

Fig. 2.2 Model of Receiver Array

CHAPTER 3

SIMULATION DETAILS AND RESULTS

3.1 The Model

The simulation implemented the following three sensor model:

$$x_1(k) = s(k-D_1) + n_1(k)$$

$$x_2(k) = s(k) \quad + n_2(k)$$

$$x_3(k) = s(k-D_3) + n_3(k) \qquad (3\text{-}1)$$

where k is the time index, and D_1 and D_3 are the time delays which were chosen to be 8 and 4 samples, respectively. As before s(k) represents the source signal, $n_i(k)$ is the additive noise at the i-th sensor, and $x_i(k)$ is the output of the i-th sensor. Two source signals were considered. In the first case the signal consisted of low-passed white Gaussian noise while the second signal consisted of bandpassed white Gaussian noise. For both signals the additive noises were uncorrelated white Gaussian noise sequences. The generation and processing of the signal and noise sequences are described in the following sections.

3.2 Generation of Signal and Noise Sequences

Four white Gaussian noise sequences with unit variances were generated using the pseudo-random number routine, GAUSS, from the KSU Signal Processing Laboratory program library. Each of the four sequences was divided into 32 equal length segments corresponding to the 32 trials performed. The MSC was then computed for each pair of the four sequences for all 32 trials to ensure the sequences were mutually incoherent and therefore mutually uncorrelated. Some typical MSC plots are shown in Figures 3.1 and 3.2.

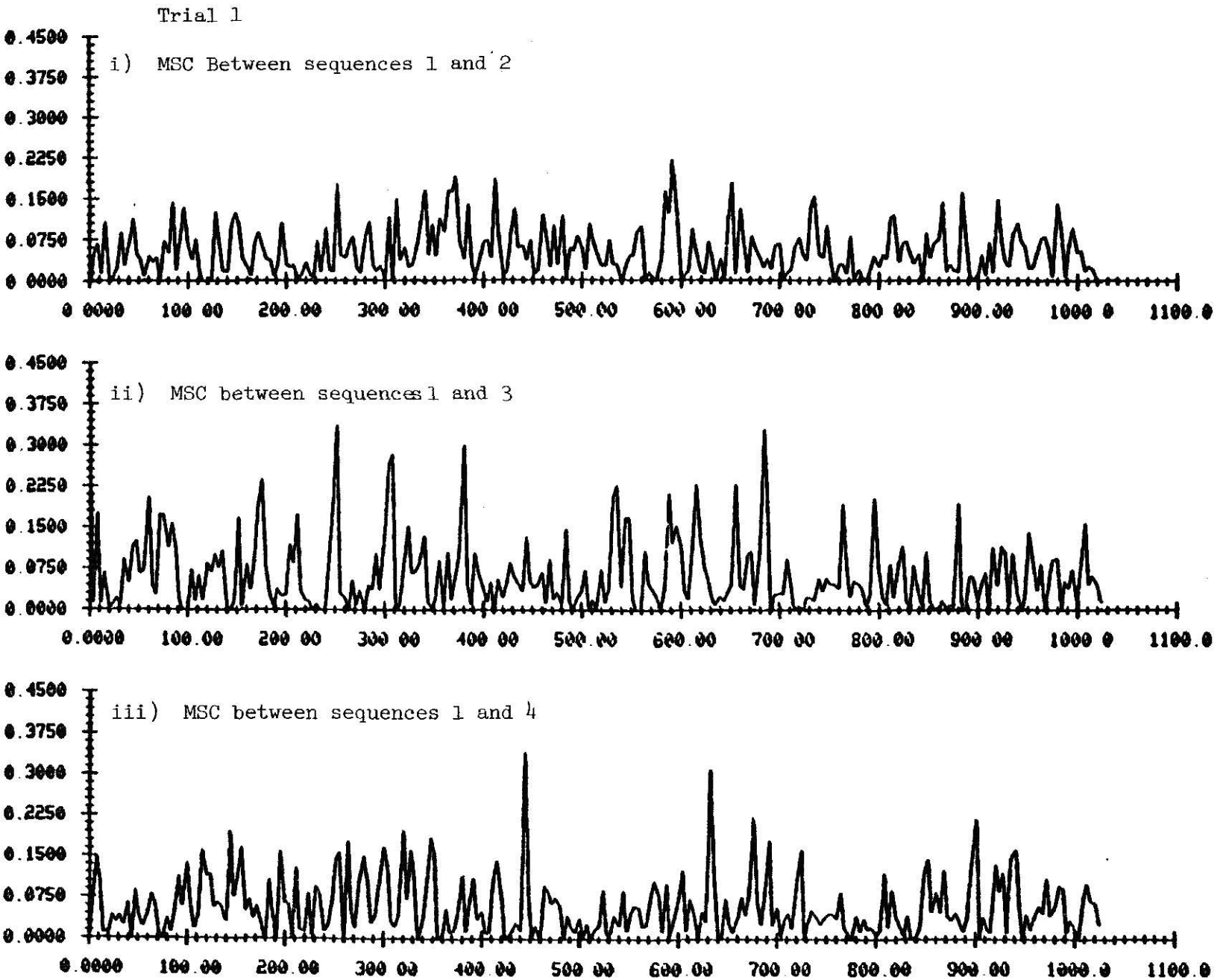
Trial 1
i) MSC Between sequences 1 and 2
0.4500
0.3750
0.3000
0.2250
0.1500
0.0750
0.0000
0.0000 100.00 200.00 300.00 400.00 500.00 600.00 700.00 800.00 900.00 1000.0 1100.0
ii) MSC between sequences 1 and 3
0.4500
0.3750
0.3000
0.2250
0.1500
0.0750
0.0000
0.0000 100.00 200.00 300.00 400.00 500.00 600.00 700.00 800.00 900.00 1000.0 1100.0
iii) MSC between sequences 1 and 4
0.4500
0.3750
0.3000
0.2250
0.1500
0.0750
0.0000
0.0000 100.00 200.00 300.00 400.00 500.00 600.00 700.00 800.00 900.00 1000.0 1100.0

Figure 3.1 (a)

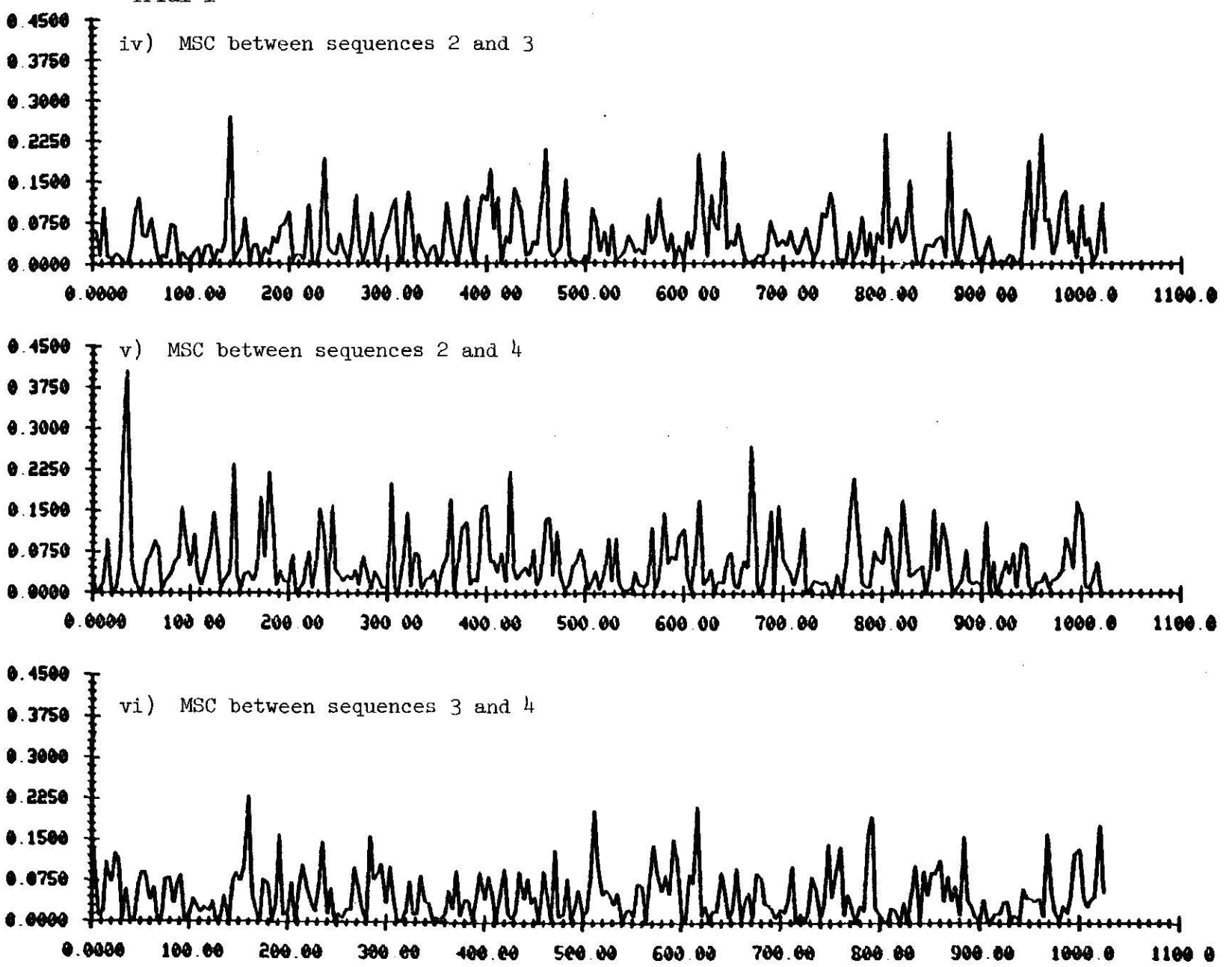
Trial 1
iv) MSC between sequences 2 and 3
v) MSC between sequences 2 and 4
vi) MSC between sequences 3 and 4
0.4500
0.3750
0.3000
0.2250
0.1500
0.0750
0.0000
0.0000
100.00
200.00
300.00
400.00
500.00
600.00
700.00
800.00
900.00
1000.0
1100.0

Figure 3.1 (b)

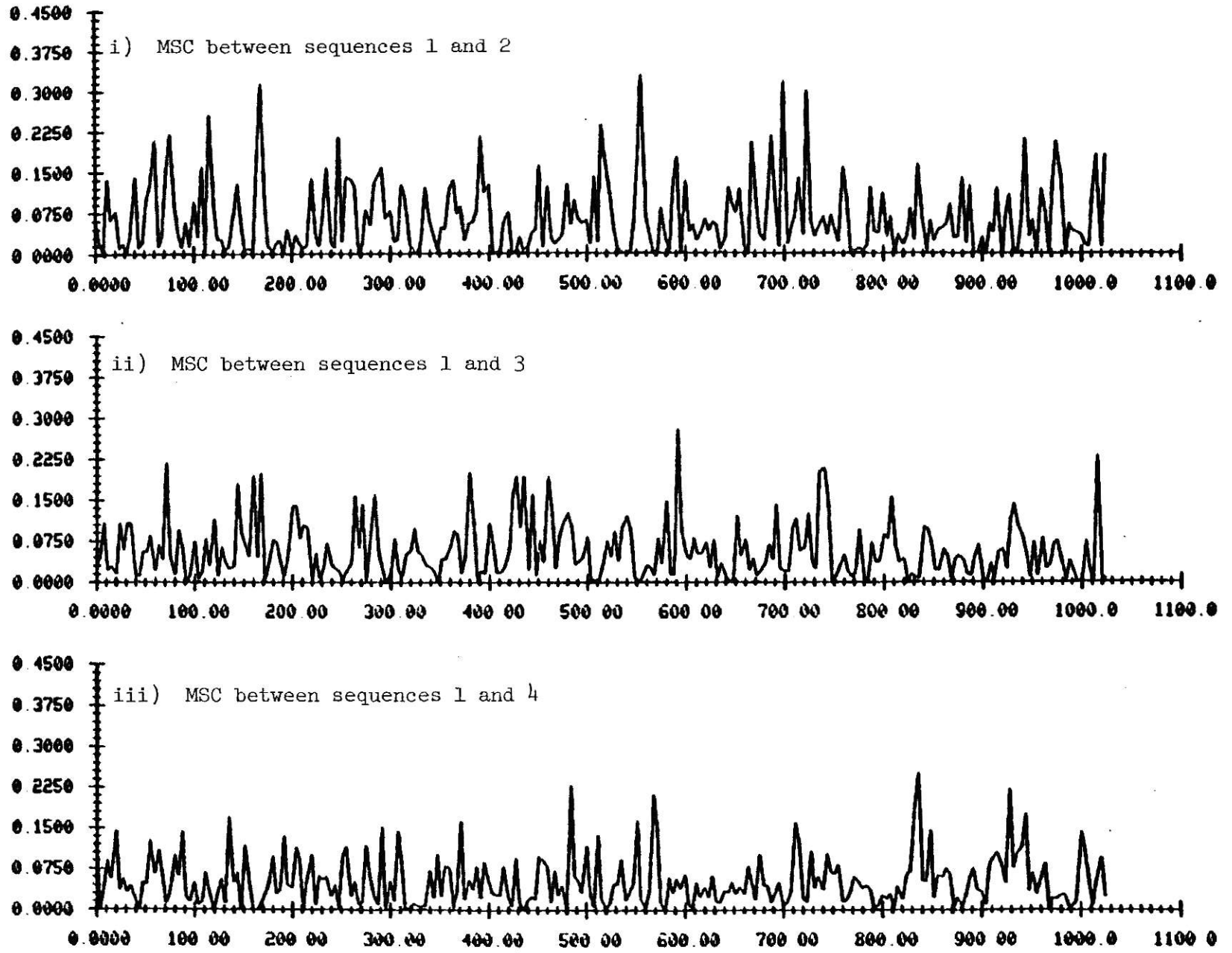
Trial 16
i) MSC between sequences 1 and 2
ii) MSC between sequences 1 and 3
iii) MSC between sequences 1 and 4
0.4500
0.3750
0.3000
0.2250
0.1500
0.0750
0.0000
0.0000
100.00
200.00
300.00
400.00
500.00
600.00
700.00
800.00
900.00
1000.0
1100.0

Figure 3.2 (a)

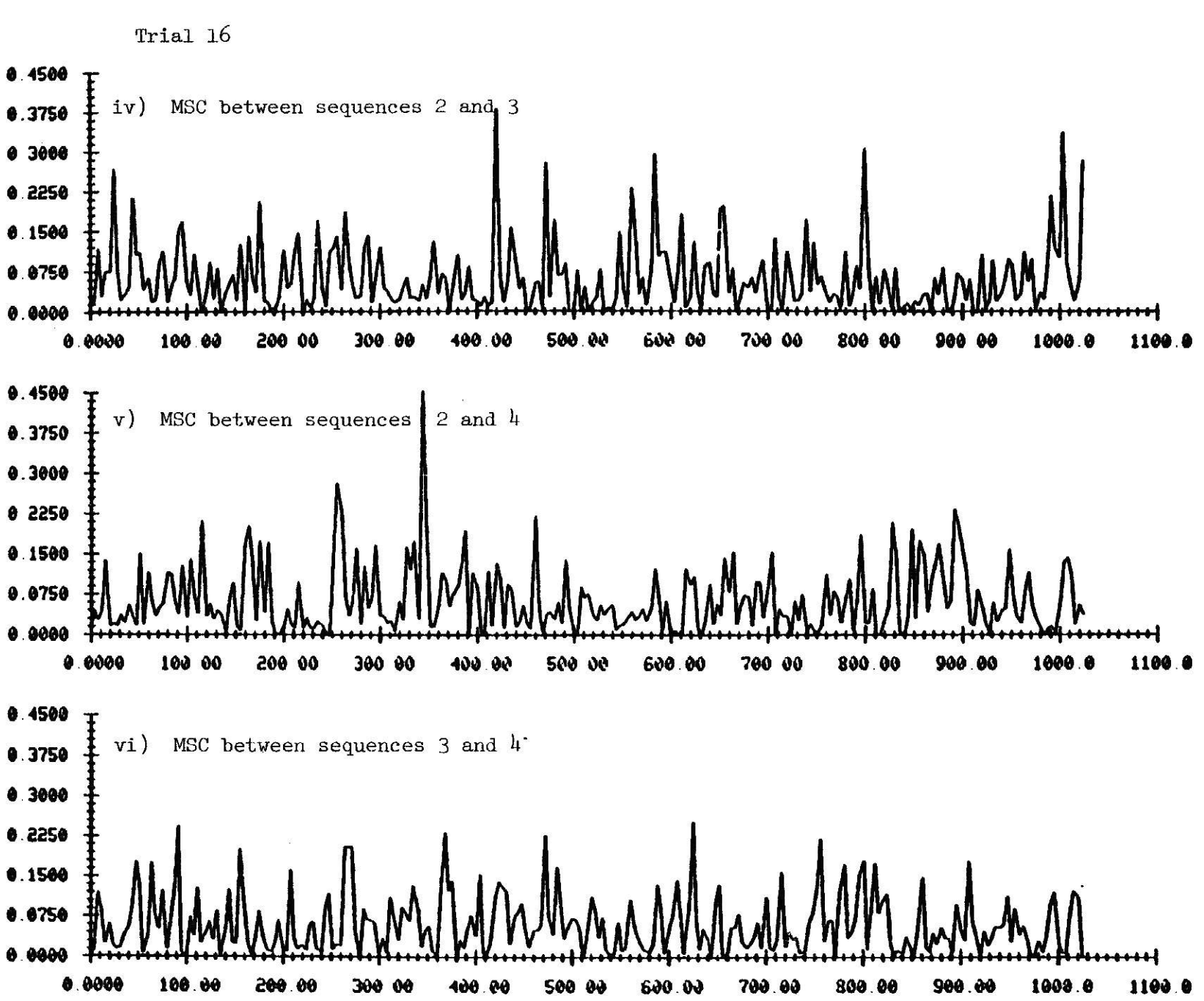
Trial 16
iv) MSC between sequences 2 and 3
v) MSC between sequences 2 and 4
vi) MSC between sequences 3 and 4
0.4500
0.3750
0.3000
0.2250
0.1500
0.0750
0.0000
0.0000
100.00
200.00
300.00
400.00
500.00
600.00
700.00
800.00
900.00
1000.0
1100.0

Figure 3.2 (b)

Three of these four white Gaussian noise sequences were used to represent the additive noises, $n_1(k)$, $n_2(k)$ and $n_3(k)$, at the remote sensors. The fourth sequence was passed through two digital filters $H_1(z)$ and $H_2(z)$ which had the following characteristics:

$$|H_1(f)| \simeq \begin{cases} 1; & 0 \leq f \leq 100 \text{ Hz} \\ 0; & \text{elsewhere} \end{cases}$$
$$|H_2(f)| \simeq \begin{cases} 1; & 100 \leq f \leq 200 \text{ Hz} \\ 0; & \text{elsewhere} \end{cases} \qquad (3\text{-}2)$$

The filter characteristics in (3-2) were realized via five second-order Butterworth sections. The resulting outputs were thus low-passed and bandpassed sequences which were used to represent the two signal sequences. These sequences were then scaled by a factor of 3.2 to again obtain unit variances. Thus the signal to noise ratio (SNR) was approximately unity; i.e.,

$$\text{SNR} = \frac{\text{Variance of source sequence}}{\text{Variance of noise sequence}} \simeq 1. \qquad (3\text{-}3)$$

Also the mean values of both the source and noise sequences were approximately zero. The source sequences were added to the noise sequences as indicated in (3-1) to obtain the remote sensor outputs, $x_1(k)$, $x_2(k)$ and $x_3(k)$.

3.3 Processing of Sensor Outputs

The sensor outputs were processed two at a time to estimate the time delays between sensors 1 and 2 and sensors 2 and 3. The processing was done using a "Coherence and Spectral Estimation" program developed by Carter et. al. [11], which was adapted for use on the NOVA 1200 system at KSU. As stated previously 32 trials were conducted during the simulation. For each trial the input sequences were processed as 16 disjoint segments of 512 points each, with the sampling frequency

taken to be 2048 Hz. Thus each trial represents 512 x 16/2048 = 4 seconds of data in real time. It is noted here that while the data was processed as disjoint segments in the simulation, it may be desirable to use overlapped segments in practice as discussed in [12].

The data segments were smoothed by a raised cosine window and then the Fast Fourier Transform (FFT) was computed via Singleton's algorithm [13] to obtain estimates of the auto and cross power spectral densities for each segment. These values were then averaged to obtain an estimate of the true power spectra and the corresponding MSC was computed for each trial. These estimates were used in turn to compute the generalized cross correlation functions. This was accomplished by multiplying the cross power spectral estimate by the appropriate weighting function and taking the inverse FFT as discussed in Chapter 2. The weighting function used for the basic cross correlation function was W(f)=1, while those for the SCOT and AML functions are given in (2-6) and (2-12) respectively. These computations were carried out for both the low-passed and bandpassed signals. Finally an idealized correlation function was obtained using the weighting functions

$$W_1(f) = \begin{cases} 1; & 0 \le f \le 100 \text{ Hz} \\ 0; & \text{elsewhere} \end{cases}$$

$$W_2(f) = \begin{cases} 1; & 100 \le f \le 200 \text{ Hz} \\ 0; & \text{elsewhere} \end{cases} \qquad (3\text{-}4)$$

where $W_1(f)$ and $W_2(f)$ correspond to the low-passed and bandpassed cases, respectively. The motivation for doing so was to determine the effect of non-zero weighting in regions of the frequency domain where the signal power was zero.

The above cross correlation functions, (say $\hat{R}(k)$), were then plotted (See Appendix B), and the corresponding time delay estimates were determined from the argument that maximized $\hat{R}(k)$. The resulting time delay estimates were then used to estimate the range, and the corresponding means and variances were computed. These results are discussed in the next section.

3.4 Simulation Results

The results of the simulation are summarized in Table 3.1. The results for each trial for the standard cross correlation, SCOT and AML methods are presented in Tables 3.2 through 3.4, respectively. The individual trial results obtained using the optimum weighting function of (3-4) are omitted as the time delays, D_{21} and D_{32}, were predicted correctly in all 32 trials for both the low-passed and band-passed cases. The plots of these four correlation functions from which the time delay estimates were obtained are shown in Appendix B. The calculations of the theoretical variances of the time delay estimates are given in Appendix A.

For the case of the low-passed signal the AML method performed somewhat better than the cross correlation method in terms of the variances of the time delay estimates. Both the AML and the cross correlation methods achieved significantly better performance than the SCOT technique. The cross correlation method also gave fairly good agreement between the experimental and theoretical variances of the time delay estimates. The theoretical variance for the AML method (i.e. the variance of the ML processor) represents the minimum obtainable variance in theory as it has been shown [8] that the variance of the ML processor obtains the Cramer-Rao lower bound. The effect of spectral

	Low-Passed Case				Bandpassed Case			
	SCOT	Cross Corr	AML	Optimum	SCOT	Cross Corr	AML	Optimum
D_{21}	-7.59	-7.94	-7.94	-8.00	-7.97	-8.00	-8.00	-8.00
$\sigma_{D_{21}}$	1.27	0.66	0.50	0.0	0.73	0.0	0.0	0.0
$\overline{D}_{32}$	4.19	4.00	3.88	4.00	4.06	4.00	4.00	4.00
$\sigma_{D_{32}}$	1.53	0.56	0.49	0.0	0.61	0.0	0.0	0.0
$\sigma_{\Delta D}$ (theo)	7.2	0.65	0.09	0.09	1.0	0.10	0.03	0.03
$\overline{R}$ (ft)	350.9	337.2	340.1	333.2	334.6	333.2	333.2	333.2
$\sigma_{\Delta R}$	67.8	28.4	22.1	0.0	28.7	0.0	0.0	0.0
$\sigma_{\Delta R}$ (theo)	275	24.8	3.5	3.5	39.2	3.7	1.3	1.3

Table 3.1 Simulation Results
$D_{21} = -8T$, $D_{32} = 4T$, Range = 333.2 ft.

	Low-passed Case			Bandpassed Case		
Trial	D_{21}	D_{32}	Range	D_{21}	D_{32}	Range
1	-8	5	306.7	-8	4	333.2
2	-7	3	402.5	-8	4	333.2
3	-8	4	333.2	-8	4	333.2
4	-9	5	283.3	-8	4	333.2
5	-8	4	333.2	-8	4	333.2
6	-7	4	365.2	-8	4	333.2
7	-9	4	306.0	-8	4	333.2
8	-8	3	364.3	-8	4	333.2
9	-9	4	306.0	-8	4	333.2
10	-8	4	333.2	-8	4	333.2
11	-8	4	333.2	-8	4	333.2
12	-8	4	333.2	-8	4	333.2
13	-9	4	306.0	-8	4	333.2
14	-8	4	333.2	-8	4	333.2
15	-7	4	365.2	-8	4	333.2
16	-8	4	333.2	-8	4	333.2
17	-8	4	333.2	-8	4	333.2
18	-9	4	306.0	-8	4	333.2
19	-8	4	333.2	-8	4	333.2
20	-7	4	365.2	-8	4	333.2
21	-9	5	283.3	-8	4	333.2
22	-8	3	364.3	-8	4	333.2
23	-7	4	365.2	-8	4	333.2
24	-7	4	365.2	-8	4	333.2
25	-8	3	364.3	-8	4	333.2
26	-8	4	333.2	-8	4	333.2
27	-8	3	364.3	-8	4	333.2
28	-7	4	365.2	-8	4	333.2
29	-8	4	333.2	-8	4	333.2
30	-8	5	306.7	-8	4	333.2
31	-7	4	365.2	-8	4	333.2
32	-8	5	306.7	-8	4	333.2
Mean	-7.94	4.00	337.2	-8	4	333.2
Std. Dev.	0.66	0.56	28.1	0.0	0.0	0.0

σ(Range error) = 28.4

σ(Range error) = 0.0

	Low-passed Case			Bandpassed Case		
Trial	D_{21}	D_{32}	Range	D_{21}	D_{32}	Range
1	-6	5	365.6	-7	5	333.8
2	-7	3	402.5	-7	3	402.5
3	-6	6	334.0	-8	4	333.2
4	-6	5	365.6	-9	5	283.3
5	-9	6	263.5	-9	4	306.0
6	-7	4	365.2	-7	4	365.2
7	-9	6	263.5	-9	4	306.0
8	-8	3	364.3	-8	3	364.3
9	-10	4	282.5	-9	4	306.0
10	-8	2	401.3	-8	4	333.2
11	-10	6	245.6	-8	4	333.2
12	-7	5	333.8	-8	5	306.7
13	-9	4	306.0	-7	4	365.2
14	-8	9	230.5	-8	4	333.2
15	-7	1	504.4	-7	4	365.2
16	-8	4	333.2	-8	4	333.2
17	-8	3	364.3	-8	4	333.2
18	-6	4	403.3	-9	4	306.0
19	-8	4	333.2	-8	4	333.2
20	-7	4	365.2	-7	4	365.2
21	-9	5	283.3	-9	5	283.3
22	-8	3	364.3	-8	3	364.3
23	-7	4	365.2	-7	4	365.2
24	-10	4	282.5	-9	4	306.0
25	-5	3	506.8	-8	3	364.3
26	-8	4	333.2	-8	4	333.2
27	-6	3	449.0	-8	3	364.3
28	-7	4	365.2	-7	4	365.2
29	-6	5	365.6	-9	4	306.0
30	-8	5	306.7	-8	5	306.7
31	-7	5	333.8	-7	5	333.8
32	-8	1	446.3	-8	5	306.7
Mean	-7.59	4.19	350.9	-7.97	4.06	334.6
Std. Dev.	1.27	1.53	65.5	0.73	0.61	28.6
	σ(Range error) = 67.8			σ(Range error) = 28.7		

Table 3.3 SCOT Results

	Low-passed Case			Bandpassed Case		
Trial	D_{21}	D_{32}	Range	D_{21}	D_{32}	Range
1	-8	3	364.3	-8	4	333.2
2	-7	3	402.5	-8	4	333.2
3	-7	4	365.2	-8	4	333.2
4	-9	4	306.0	-8	4	333.2
5	-8	4	333.2	-8	4	333.2
6	-7	4	365.2	-8	4	333.2
7	-9	4	306.0	-8	4	333.2
8	-8	5	306.7	-8	4	333.2
9	-7	4	365.2	-8	4	333.2
10	-8	4	333.2	-8	4	333.2
11	-8	4	333.2	-8	4	333.2
12	-8	3	364.3	-8	4	333.2
13	-8	4	333.2	-8	4	333.2
14	-8	4	333.2	-8	4	333.2
15	-8	4	333.2	-8	4	333.2
16	-8	4	333.2	-8	4	333.2
17	-8	4	333.2	-8	4	333.2
18	-8	4	333.2	-8	4	333.2
19	-8	4	333.2	-8	4	333.2
20	-8	4	333.2	-8	4	333.2
21	-8	4	333.2	-8	4	333.2
22	-8	5	306.7	-8	4	333.2
23	-8	4	333.2	-8	4	333.2
24	-8	4	333.2	-8	4	333.2
25	-8	3	364.3	-8	4	333.2
26	-8	4	333.2	-8	4	333.2
27	-8	4	333.2	-8	4	333.2
28	-8	4	333.2	-8	4	333.2
29	-9	3	332.2	-8	4	333.2
30	-8	4	333.2	-8	4	333.2
31	-7	4	365.2	-8	4	333.2
32	-8	3	364.3	-8	4	333.2
Mean	-7.94	3.88	340.1	-8	4	333.2
Std. Dev.	0.50	0.49	21.7	0.0	0.0	0.0
	σ(Range error) = 22.1			σ(Range error) = 0.0		

Table 3.4 AML Results

value for the experimental variance of the time delay estimates. The best performance was obtained using the optimum weighting function as expected, when the time delays were estimated correctly in every trial. As can be seen from the experimental values for the variance of the time delay estimates, the sub-optimum weightings of the other techniques caused a degradation in performance.

For the bandpassed signal the AML method, the cross correlation method, and the processor using the optimum weighting function all correctly estimated the time delays in all 32 trials. This improved performance was expected based on the smaller values obtained for the theoretical variances of the time delay estimates. The SCOT method also performed better for the bandpassed signal than for the low-passed signal, but again showed poorer performance than the other techniques. Using the 32 estimates of the time delays, D_{21} and D_{32}, 32 estimates of the range were computed as in (2-16) using the values $L_1=L_2=100$ ft and $C = 5000$ ft/sec. These values are also given in Tables 3.2-3.4. In addition, the variance of the range error was computed from(2-17) with $L_e = 100$ ft, and the theoretical variance of the time delay estimate was used for $\sigma^2_{D_{31}}$. From Table 3.1 it is seen that good agreement between the experimental and theoretical variances of the range error was obtained for the low-passed cross correlation case. However, there was relatively poor agreement for the SCOT method where the theoretical variance is larger than that obtained from the simulation, for both the low-passed and bandpassed signals. For those cases in which the time delays were correctly estimated in all 32 trials, thus yielding zero variance for the range

error, the theoretical variances were so small that more trials would be required to compare the experimental and theoretical values.

CHAPTER 4

CONCLUSIONS

This work has presented the results of a simulation comparing the performances of the standard cross correlation, the AML and the SCOT methods of estimating the time delays between signals corrupted by noise received at three remote sensors. The time delay estimates so obtained were used to compute estimates of the range of the source. Also, the theoretical variances of the time delay estimates and range error were computed and compared to those obtained experimentally. It was shown that for the case of a narrow band Gaussian signal embedded in white Gaussian noise, both the standard cross correlation and the AML methods perform significantly better than the SCOT method. This is in agreement with the simulation results of Hassab and Boucher as given in [14]. However, it should be noted that for certain types of input data the SCOT method has been shown to outperform the standard cross correlation method [3].

Further simulation work could include using fewer disjoint segments to estimate the power spectra, different signal to noise ratios and different bandwidths for the signal sequence. Another area that merits a detailed investigation is the case of a moving source. Some effort in this direction has been initiated recently [15].

ACKNOWLEDGEMENT

I would like to thank my friends and family, especially my parents, for their support of my academic endeavors.

I also wish to express my appreciation to Dr. Donald R. Hummels and Dr. David Logan for being members of my graduate committee and for their advice and assistance. I particularly want to thank my major advisor, Dr. Nasir Ahmed, and Dr. G. Clifford Carter of the Naval Underwater Systems Center, New London, CT for their invaluable support and guidance.

REFERENCES

[1] G.C. Carter, "Passive ranging errors due to receiving hydrophone position uncertainty", J. Acoust. Soc. Am., 65(2), pp 528-530, Feb. 1979.

[2] P.R. Roth, "Effective measurements using digital signal analysis", IEEE Spectrum, Vol. 8, pp 62-70, Apr. 1971

[3] G.C. Carter, A.H. Nuttall, and P.G. Cable, "The smoothed coherence transform", Proc. IEEE (Lett.), Vol. 61, pp. 1497-1498, Oct. 1973.

[4] G.C. Carter, A.H. Nuttall, and P.G. Cable, "The smoothed coherence transform (SCOT)", Naval Underwater Systems Center, New London, CT., Tech. Memo TL-159-72, Aug. 8 1972.

[5] C. Eckart, "Optimal rectifier systems for detection of steady signals", Univ. of California, Scripps Inst. Oceanography, Marine Physical Lab., Rep. SIO 12692, SIO Ref. 52-11, 1952.

[6] C.H. Knapp and G.C. Carter, "The generalized correlation method for estimation of time delay ", IEEE Trans. Acous., Speech, and Signal Proc., Vol ASSP-24, No. 4, pp. 320-327, Aug. 1976.

[7] E.J. Hannan and P.J. Thomson, "The estimation of coherence and group delay", Biometrika, Vol. 58, pp. 469-481, 1971.

[8] G.C. Carter, "Time Delay Estimation", Univ. of Conn., Ph.D. Thesis (1976), (available as NUSC TR 5335 through NTIS under AD# A025408).

[9] W.B. Davenport, Jr., Probability and Random Processes, New York: McGraw-Hill, 1970.

[10] G.C. Carter, "Sonar signal processing for source state estimation", EASCON 1979 record, IEEE pub. no. 79GH1476-IAES.

[11] Programs For Digital Signal Processing, Edited by the Digital Signal Processing Committee, IEEE Acoustics. Speech and Signal Processing Society, IEEE Press, 1979.

[12] G.C. Carter, C.H. Knapp and A.H. Nuttall, "Estimation of the magnitude squared coherence function via overlapped fast Fourier transform processing", IEEE Trans. Audio Electroacoust., Vol. Au-21, pp. 337-344, Aug. 1973.

[13] R.C. Singleton, "An algorithm for computing the mixed radix fast Fourier transform", IEEE Trans. Audio Electroacoust., Vol. Au-17 pp. 93-103, June 1969.

[14] J.C. Hassab and R.E. Boucher, "A quantitative study of optimum and sub-optimum filters in the generalized correlator", in Proc. 1979 IEEE Int. Conf. Acoust., Speech and Signal Proc., pp. 124-127, 1979.

[15] N. Ahmed and K. Scarbrough, "Performance evaluation of a method for time delay estimation related to moving sources", NUSC contract, Oct. 1, 1979 - Sept. 30, 1980.

APPENDIX A

CALCULATION OF THEORETICAL VARIANCES

A.1 Variance of the Time Delay Estimates

From (2-15) the theoretical variance of the time delay estimate is given by

$$\sigma^2_{\Delta D} = \frac{\int_{-\infty}^{\infty} |W(f)|^2 \, G_{x_1x_1}(f) \, G_{x_2x_2}(f)[1-C_{x_1x_2}(f)](2\pi f)^2 \, df}{T\left[\int_{-\infty}^{\infty} |W(f)| \, |G_{x_1x_2}(f)| \, (2\pi f)^2 \, df\right]^2} . \quad \text{(A-1)}$$

In the simulation the sampling frequency was 2048 Hz. Hence the limits of integration in (A1) are -1024 Hz to 1024 Hz. The observation time T was 4 seconds. To simplify the notation let $G_{11} = G_{x_1x_1}$, $G_{22} = G_{x_2x_2}$, $G_{12} = G_{x_1x_2}$ and $C_{12} = C_{x_1x_2}$. Then with some additional simplification, (A-1)becomes

$$\sigma^2_{\Delta D} = \frac{\int_0^{1024} |W(f)|^2 \, G_{11}(f) \, G_{22}(f) \, [1-C_{12}(f)] \, f^2 \, df}{8\pi^2 \, T\left[\int_0^{1024} |W(f)| \, |G_{12}(f)| \, f^2 \, df\right]^2} . \quad \text{(A-2)}$$

Thus the auto and cross power spectral densities, the MSC and the weighting function must be known to calculate the theoretical variance of the time delay estimate. Note that since the sensor outputs in (3-1) are identical (i.e., statistically), the value of $\sigma^2_{\Delta D}$ in (A-2) is independent of which two sensor outputs are considered, i.e.;

$$\sigma^2_{\Delta D} = \sigma^2_{D_{21}} = \sigma^2_{D_{32}} = \sigma^2_{D_{31}} .$$

The auto power spectra are given by

$$G_{11}(f) = G_{22}(f) = G_s(f) + G_n(f) \quad \text{(A-3)}$$

where $G_s(f)$ and $G_n(f)$ denote the power spectral densities of the signal and noise sequences, respectively. Implicit in (A-3) is the assumption that the signal and noise sequences are uncorrelated. The noise sequences are white so that

$$G_n(f) = \begin{cases} \text{constant}, & -1024 \le f \le 1024 \text{ Hz} \\ 0 & , \text{ elsewhere} \end{cases} . \tag{A-4}$$

Also recall that the noise sequences have unit variances and zero means, and thus

$$\sigma_n^2 = 1 = R_n(0) = \int_{-1024}^{1024} G_n(f)\, df \tag{A-5}$$

where R_n denotes the autocorrelation function of the noise sequence. Solving for $G_n(f)$ yields

$$G_n(f) = \begin{cases} 4.9 \times 10^{-4} \ (-33.1 \text{ dB}), & -1024 \le f \le 1024 \text{ Hz} \\ 0 & , \text{ elsewhere} \end{cases} . \tag{A-6}$$

The signal sequence consists of low-passed or bandpassed white noise and also has unit variance and zero mean. For the low-passed sequence one obtains

$$G_s(f) = \begin{cases} 5.0 \times 10^{-3} \ (-23.0 \text{ dB}) & ; -100 \le f \le 100 \text{ Hz} \\ 0 & , \text{ elsewhere} \end{cases} . \tag{A-7}$$

Thus the auto power spectra are given by

$$G_{11}(f) = G_{22}(f) = \begin{cases} 5.5 \times 10^{-3}; & 0 \le |f| \le 100 \text{ Hz} \\ 4.9 \times 10^{-4}; & 100 \le |f| \le 1024 \text{ Hz}. \end{cases} \tag{A-8}$$

The signal to noise ratio can be calculated using the values from (A-6) and (A-7) as

$$\text{SNR} = \frac{G_s(f)}{G_n(f)} = \begin{cases} 10.2; & 0 \le |f| \le 100 \text{ Hz} \\ 0 & ; \text{ elsewhere} \end{cases} \tag{A-9}$$

Equivalently the SNR can be expressed in terms of the MSC as [8]

$$\text{SNR} = \frac{\sqrt{C_{12}(f)}}{1 - \sqrt{C_{12}(f)}} \quad . \tag{A-10}$$

Solving for $C_{12}(f)$ yields

$$C_{12}(f) = \begin{cases} 0.83, & 0 \leq |f| \leq 100 \text{ Hz} \\ 0, & \text{elsewhere} \end{cases} \quad . \tag{A-11}$$

The magnitude of the cross power spectrum can then be obtained from the relation

$$C_{12}(f) = \frac{|G_{12}(f)|^2}{G_{11}(f)\, G_{22}(f)} \tag{A-12}$$

and one finds

$$|G_{12}(f)| = \begin{cases} 5.0 \times 10^{-3}, & 0 \leq |f| \leq 100 \text{ Hz} \\ 0, & \text{elsewhere} \end{cases} \quad . \tag{A-13}$$

Similarly for the bandpassed case the following values are obtained:

$$G_{11}(f) = G_{22}(f) = \begin{cases} 5.5 \times 10^{-3}, & 100 \leq |f| \leq 200 \text{ Hz} \\ 4.9 \times 10^{-4}, & \text{elsewhere} \end{cases} \quad , \tag{A-14}$$

$$C_{12}(f) = \begin{cases} 0.83 & 100 \leq |f| \leq 200 \text{ Hz} \\ 0, & \text{elsewhere} \end{cases} \quad , \tag{A-15}$$

and

$$|G_{12}(f)| = \begin{cases} 5.0 \times 10^{-3}, & 100 \leq |f| \leq 200 \text{ Hz} \\ 0, & \text{elswhere} \end{cases} \quad . \tag{A-16}$$

A.1.1 Cross Correlation Method

The weighting function for the standard cross correlation method is $W(f) = 1$. Substituting for $C_{12}(f)$ from (A-11) and for $W(f)$ in (A-2) yields

$$\sigma^2_{\Delta D} = \frac{0.17 \int_0^{100} G_{11}(f)\, G_{22}(f)\, f^2\, df + \int_{100}^{1024} G_{11}(f)\, G_{22}(f)\, f^2\, df}{8\pi^2\, T \left[\int_0^{1024} |G_{12}(f)| f^2\, df \right]^2} \qquad \text{(A-18)}$$

for the low-passed case. Substituting the values for the power spectra from (A-8) and (A-13) one finds $\sigma_{\Delta D} = 0.65$ samples. Similarly for the bandpassed case one obtains $\sigma_{\Delta D} = 0.10$ samples.

A.1.2 SCOT Method

The SCOT method uses the weighting function

$$W(f) = \frac{1}{\sqrt{G_{11}(f)\, G_{22}(f)}} \cdot \qquad \text{(A-19)}$$

Substituting this weighting function into (A-2) and making use of the relation (A-12) yields upon simplification

$$\sigma^2_{\Delta D} = \frac{\int_0^{1024} [1-C_{12}(f)]\, f^2\, df}{8\pi^2\, T \left[\int_0^{1024} \sqrt{C_{12}(f)}\, f^2\, df \right]^2} \cdot \qquad \text{(A-20)}$$

Thus for the low-passed case $\sigma_{\Delta D} = 7.2$ samples and for the bandpassed case $\sigma_{\Delta D} = 1.0$ samples.

A.1.3 AML Method

The weighting function corresponding to the ML estimator can be expressed as

$$W(f) = \frac{C_{12}(f)}{|G_{12}(f)|\, [1-C_{12}(f)]} \cdot \qquad \text{(A-21)}$$

Using this weighting function in (A-2) and simplifying one obtains

$$\sigma^2_{\Delta D} = \left[8\pi^2\, T \int_0^{1024} \frac{C_{12}(f)}{1 - C_{12}(f)}\, f^2\, df \right]^{-1}. \qquad \text{(A-22)}$$

This is the theoretical variance of the ML estimator which achieves the Cramer-Rao lower bound as noted in [6]. For the low-passed case one

obtains $\sigma_{\Delta D} = 0.90$ samples and for the bandpassed case $\sigma_{\Delta D} = 0.034$ samples.

A.1.4 Processor using Optimum Weighting Function

This processor applies the weighting function

$$W(f) = \begin{cases} 1, & \text{for f such that } G_s(f) \neq 0 \\ 0, & \text{for f such that } G_s(f) = 0 \end{cases} . \qquad \text{(A-23)}$$

Thus W(f) can be omitted from (A-2) and the limits of integration are determined by the power spectrum of the signal sequnce $G_s(f)$. For the low-passed case (A-2) becomes

$$\sigma^2_{\Delta D} = \frac{\int_0^{100} G_{11}(f)\, G_{22}(f) \left[1 - C_{12}(f)\right] f^2\, df}{8\pi^2\, T \left[\int_0^{100} |G_{12}(f)|\, f^2\, df\right]^2} . \qquad \text{(A-24)}$$

Since $G_{11}(f)$, $G_{22}(f)$, $|G_{12}(f)|$ and $C_{12}(f)$ are all constant over this frequency range they can be factored out of the integral. Then making use of the relation in (A-12) and simplifying yields

$$\sigma^2_{\Delta D} = \left[8\pi^2\, T \int_0^{100} \frac{C_{12}(f)}{1 - C_{12}(f)}\, f^2\, df\right]^{-1}, \qquad \text{(A-25)}$$

which is the same as the expression for the variance of the ML estimator. Thus for the low-passed case $\sigma_{\Delta D} = 0.090$ samples and for the bandpassed case the limits of integration in (A-25) are from 100 to 200 Hz and $\sigma_{\Delta D} = 0.034$ samples.

A.2. Variance of the Range Estimates

The theoretical variance of the range error can be computed from (2-17) to be

$$\sigma^2_{\Delta R} = 2 \left(\frac{R}{L_e}\right)^4 c^2\, \sigma^2_{\Delta D_{31}} . \qquad \text{(A-26)}$$

The value for $\sigma^2_{\Delta D_{31}}$ is the theoretical value of the variance of the time delay estimate as calculated in the preceding sections. The values obtained from (A-26) as well as the values for $\sigma^2_{\Delta D}$ are given in Table 3.1 for the various processors.

APPENDIX B

This appendix contains a sampling of the plots from which the values for the time delay estimates were obtained. Examples of the plots of the entire correlation functions for the first two trials are included followed by expanded versions of the plots for several more of the trials.

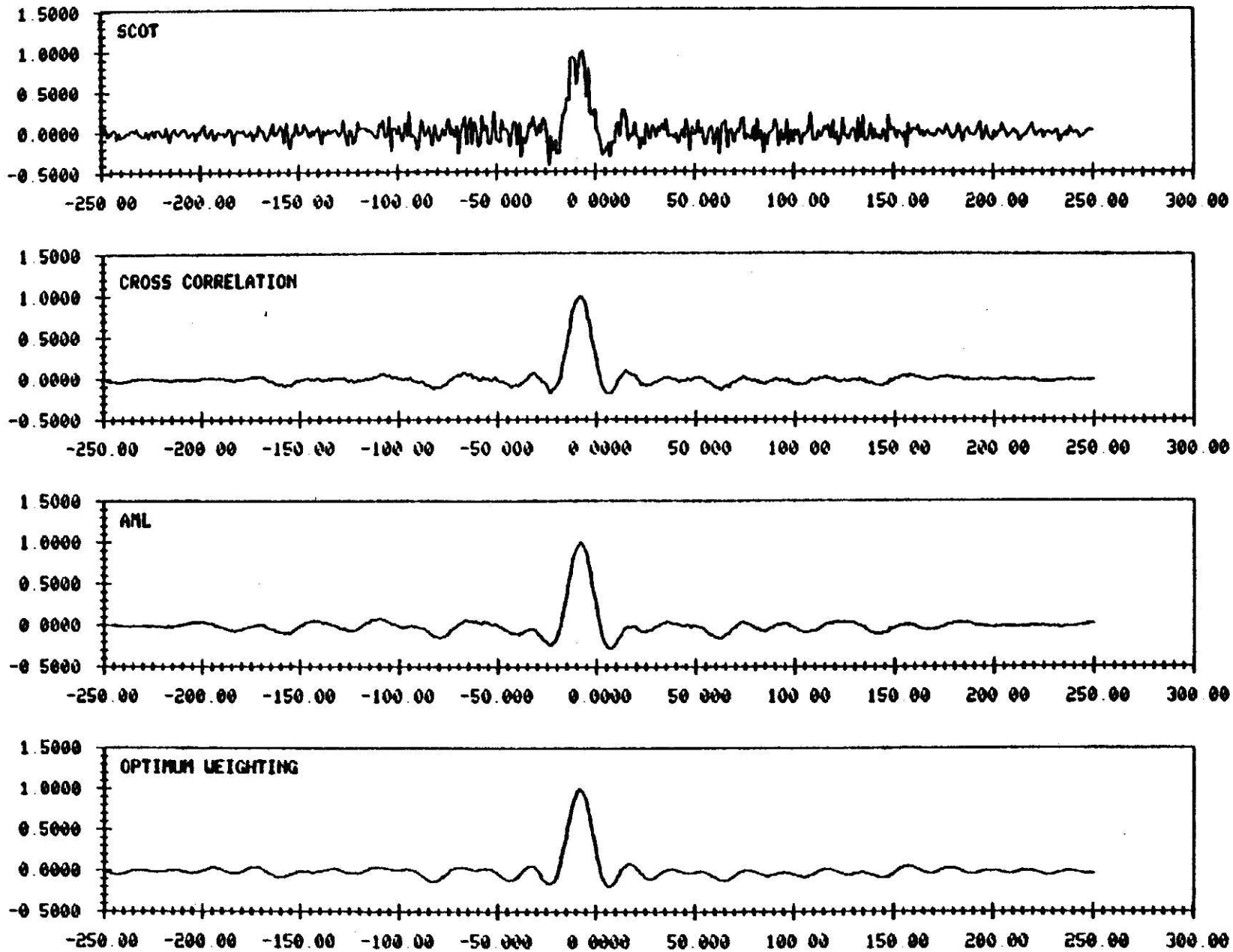

LOW-PASSED CASE - D21--8T - TRIAL 1

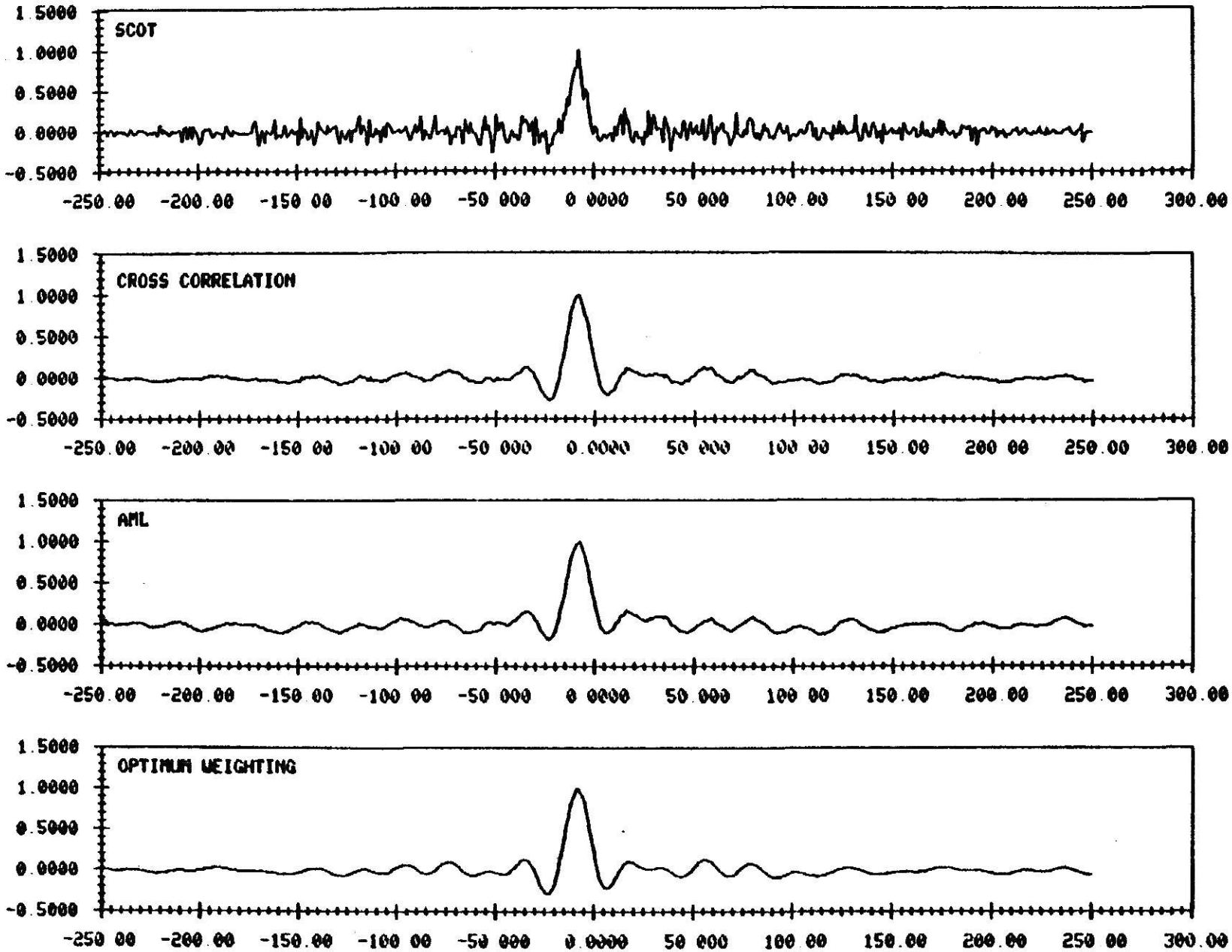

LOW-PASSED CASE - D21--8T - TRIAL 2

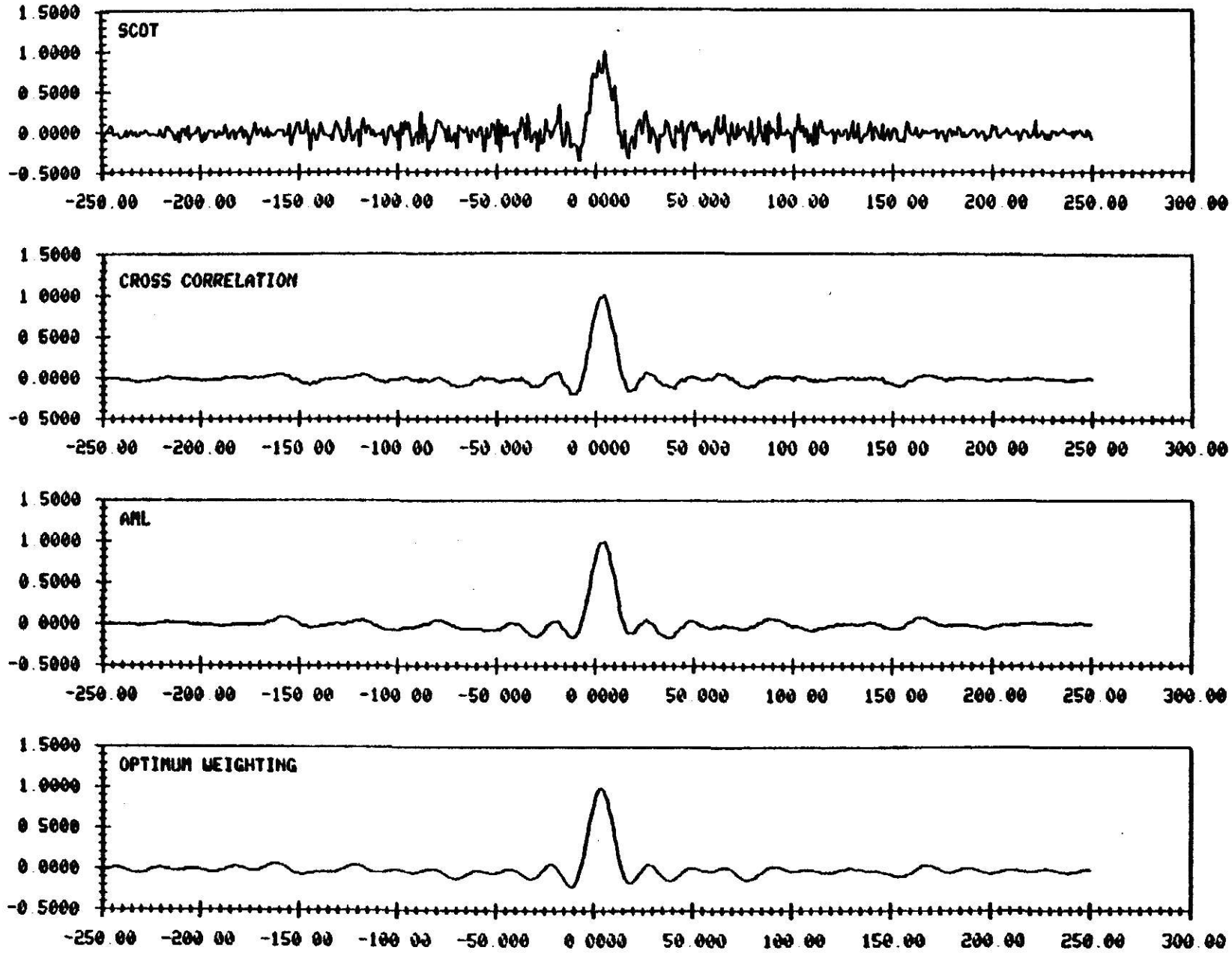

LOW-PASSED CASE - D32-4T - TRIAL 1

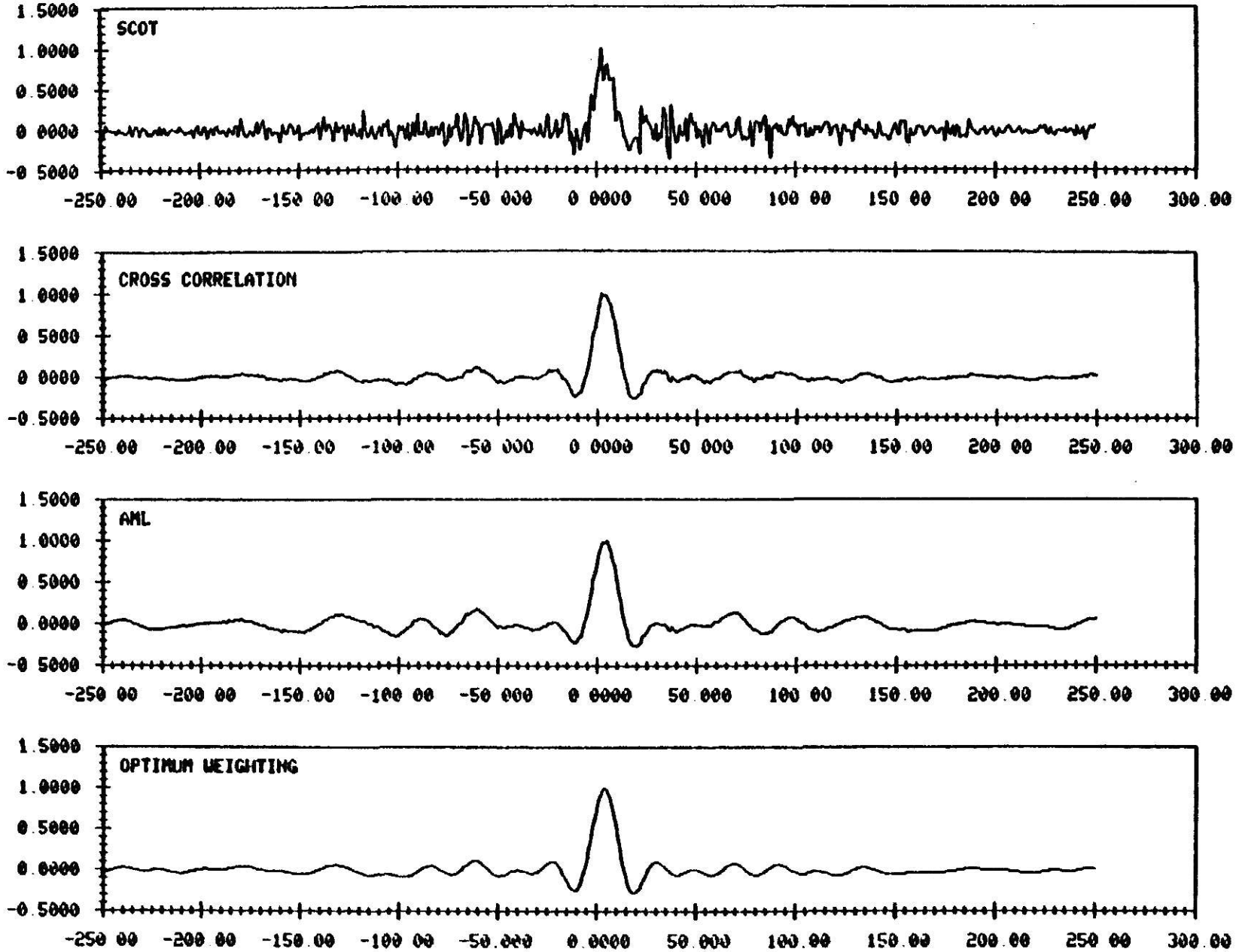

LOW-PASSED CASE - D32-4T - TRIAL 2

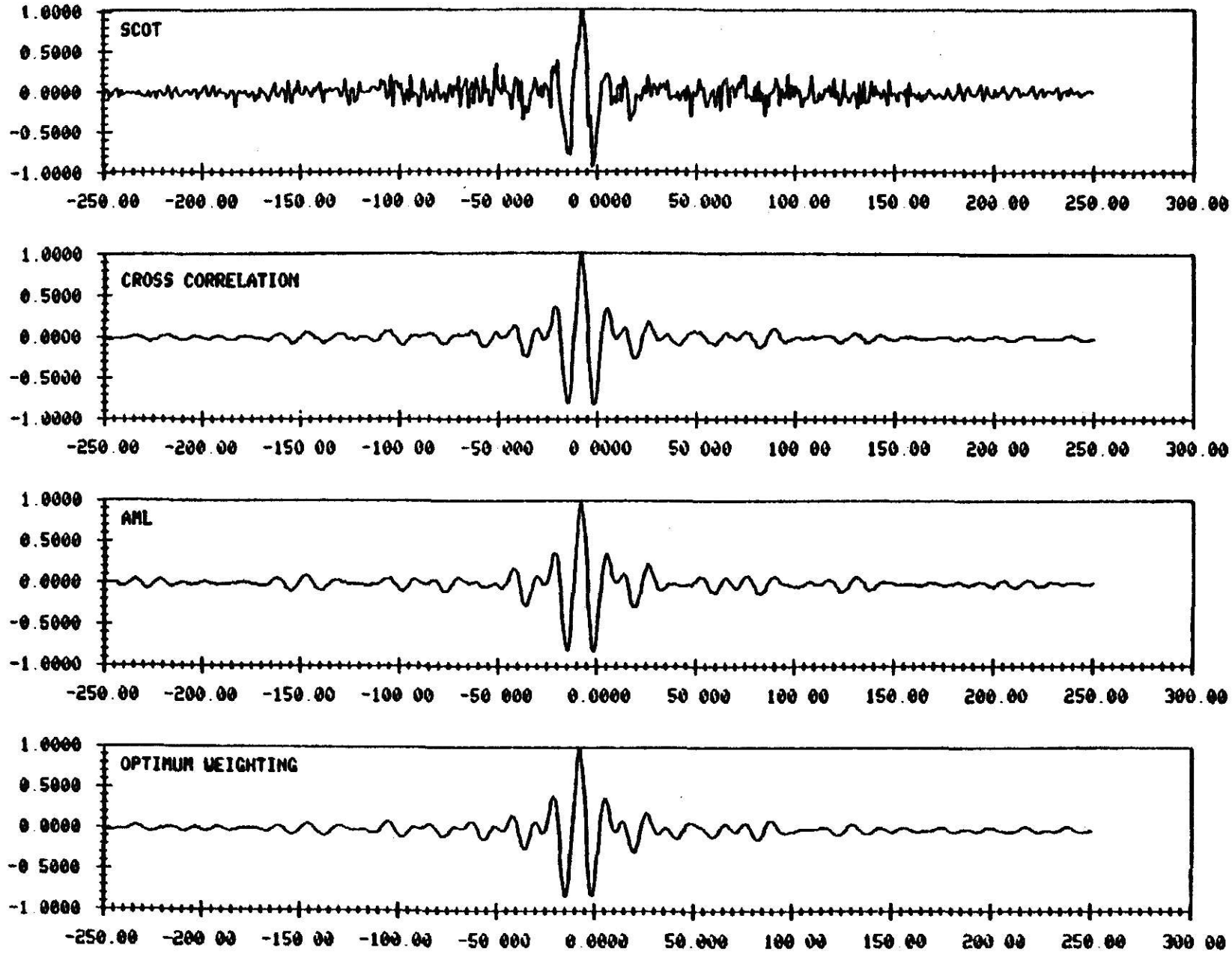

BANDPASSED CASE - D21--8T - TRIAL 1

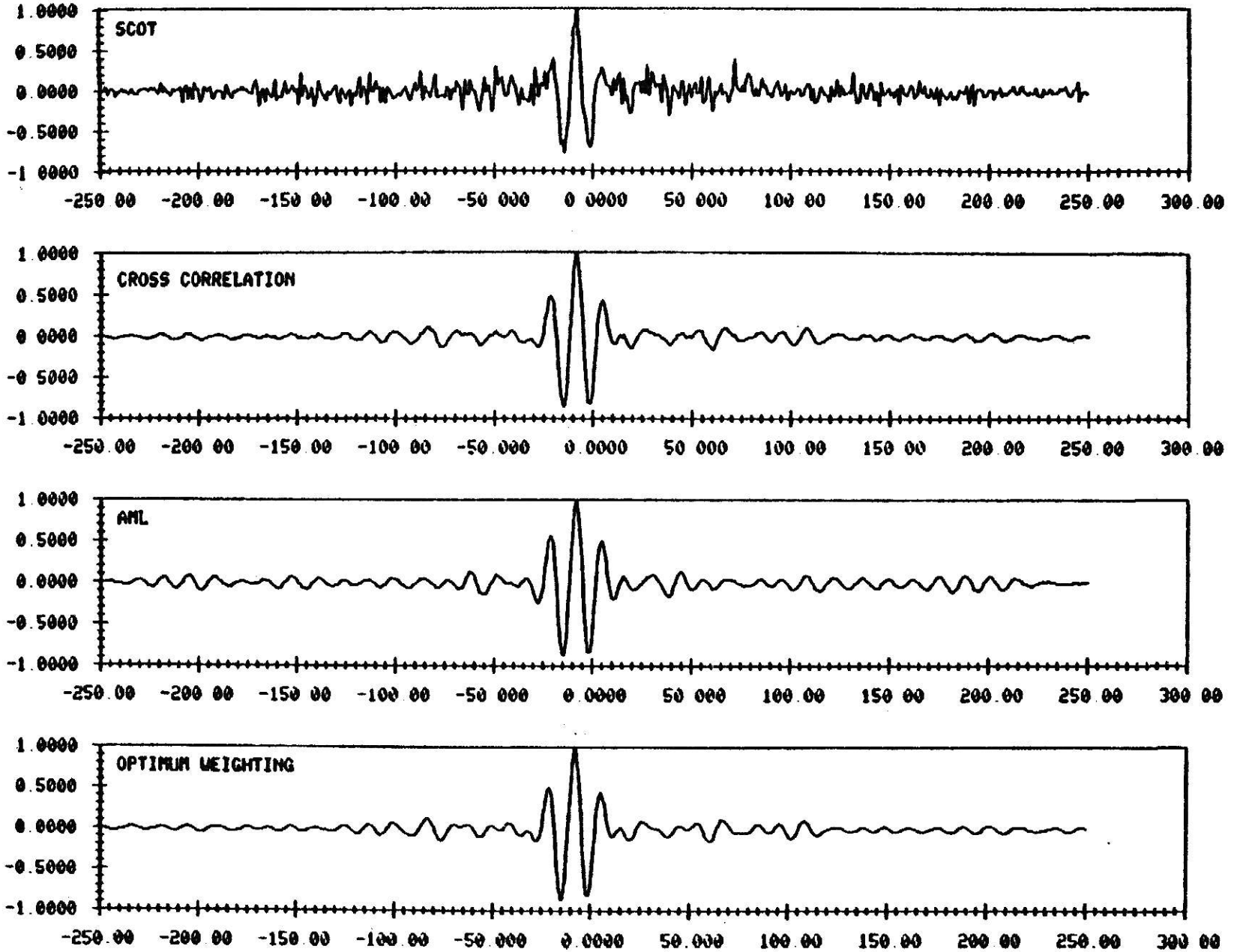

BANDPASSED CASE - D21--8T - TRIAL 2

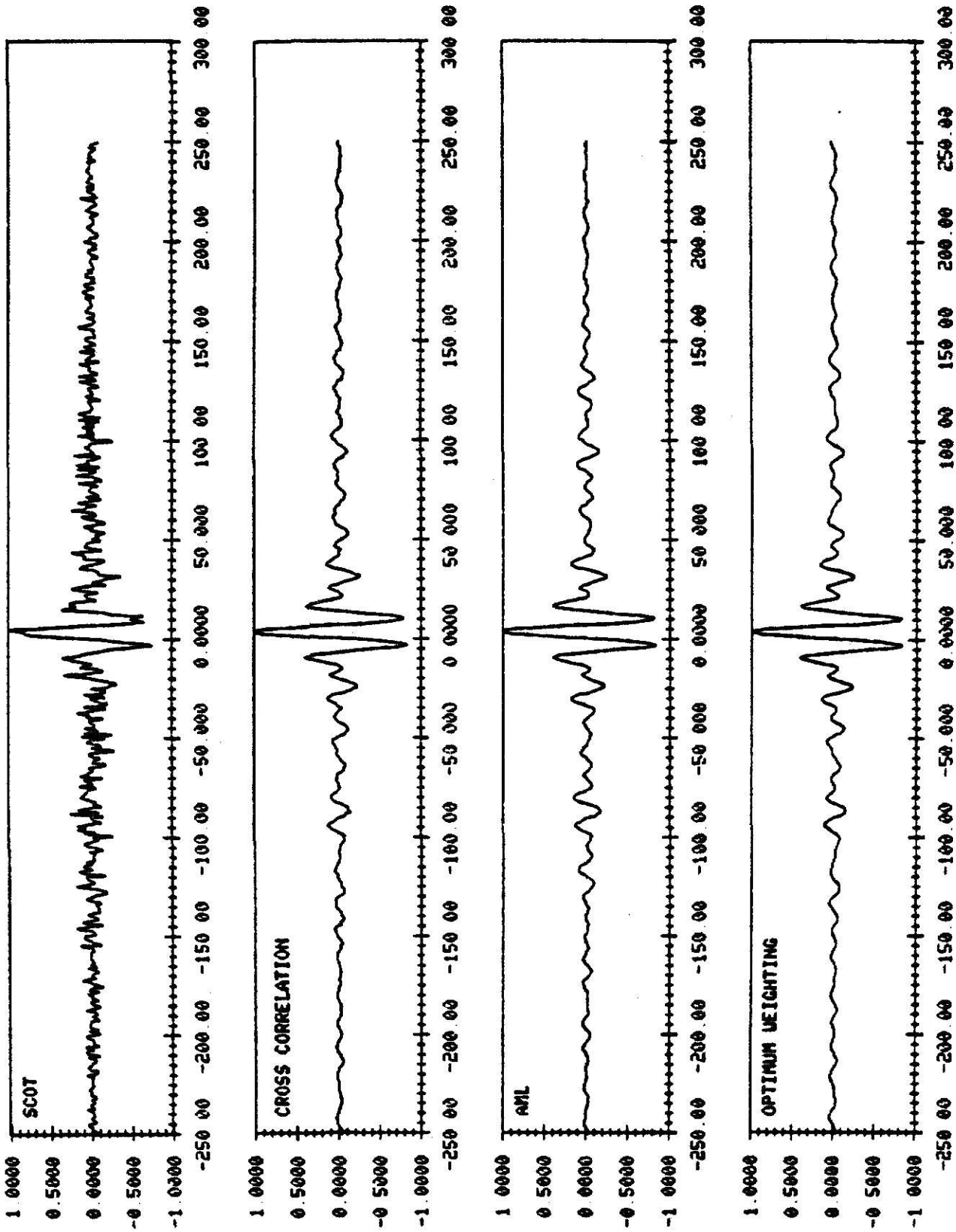

BANDPASSED CASE - D32-4T - TRIAL 1

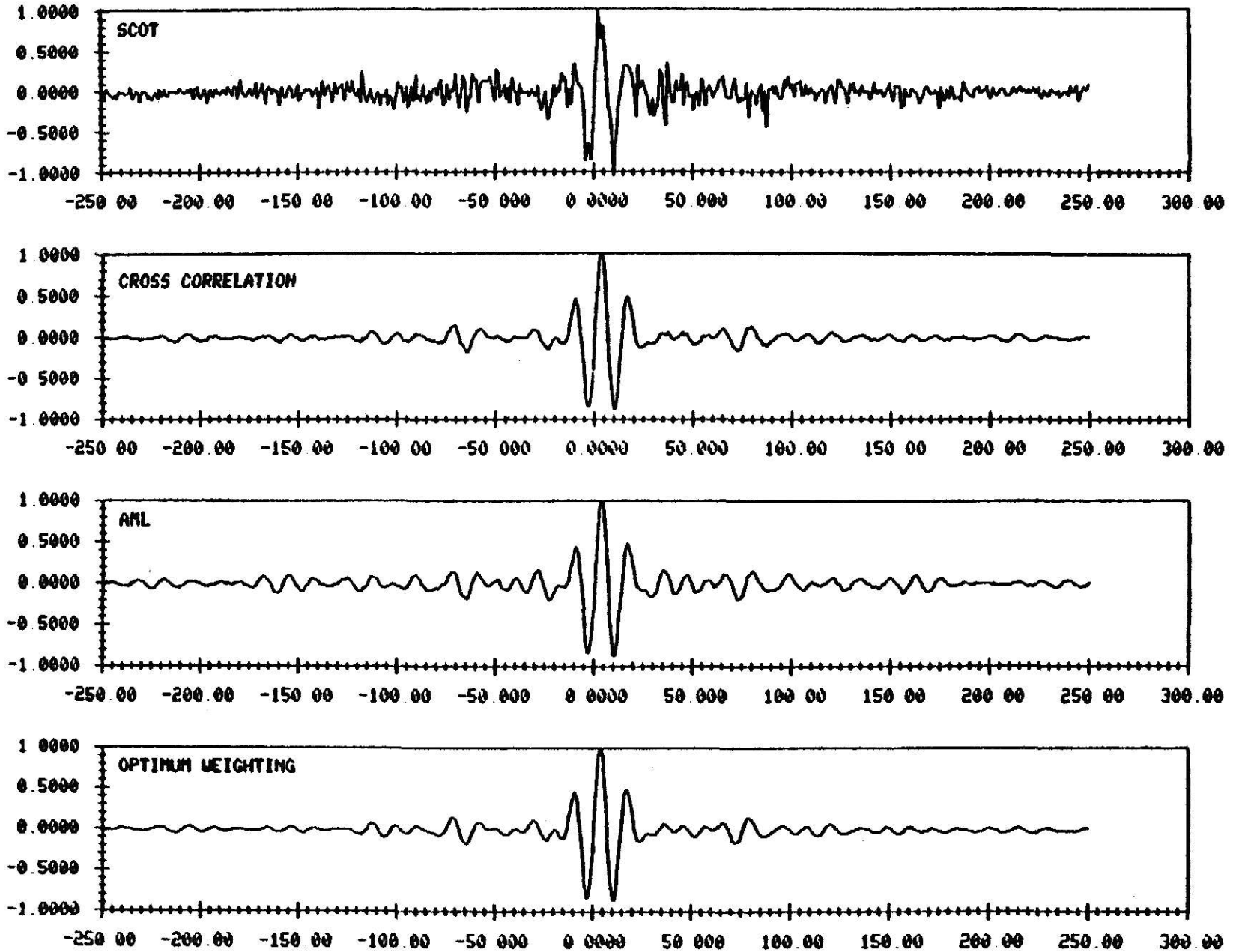

BANDPASSED CASE - B32-4T - TRIAL 2

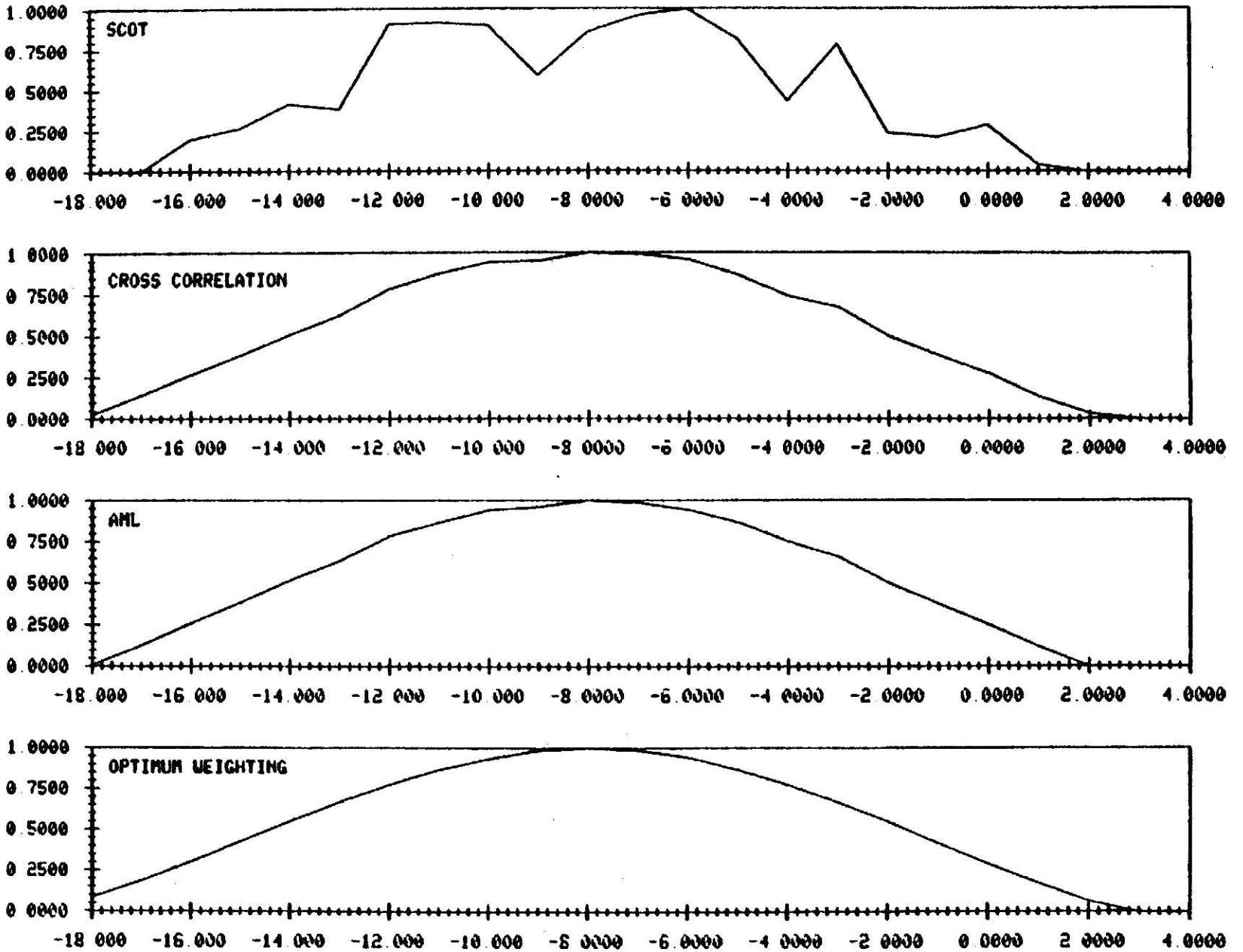

LOW-PASSED CASE - D21--8T - TRIAL 1

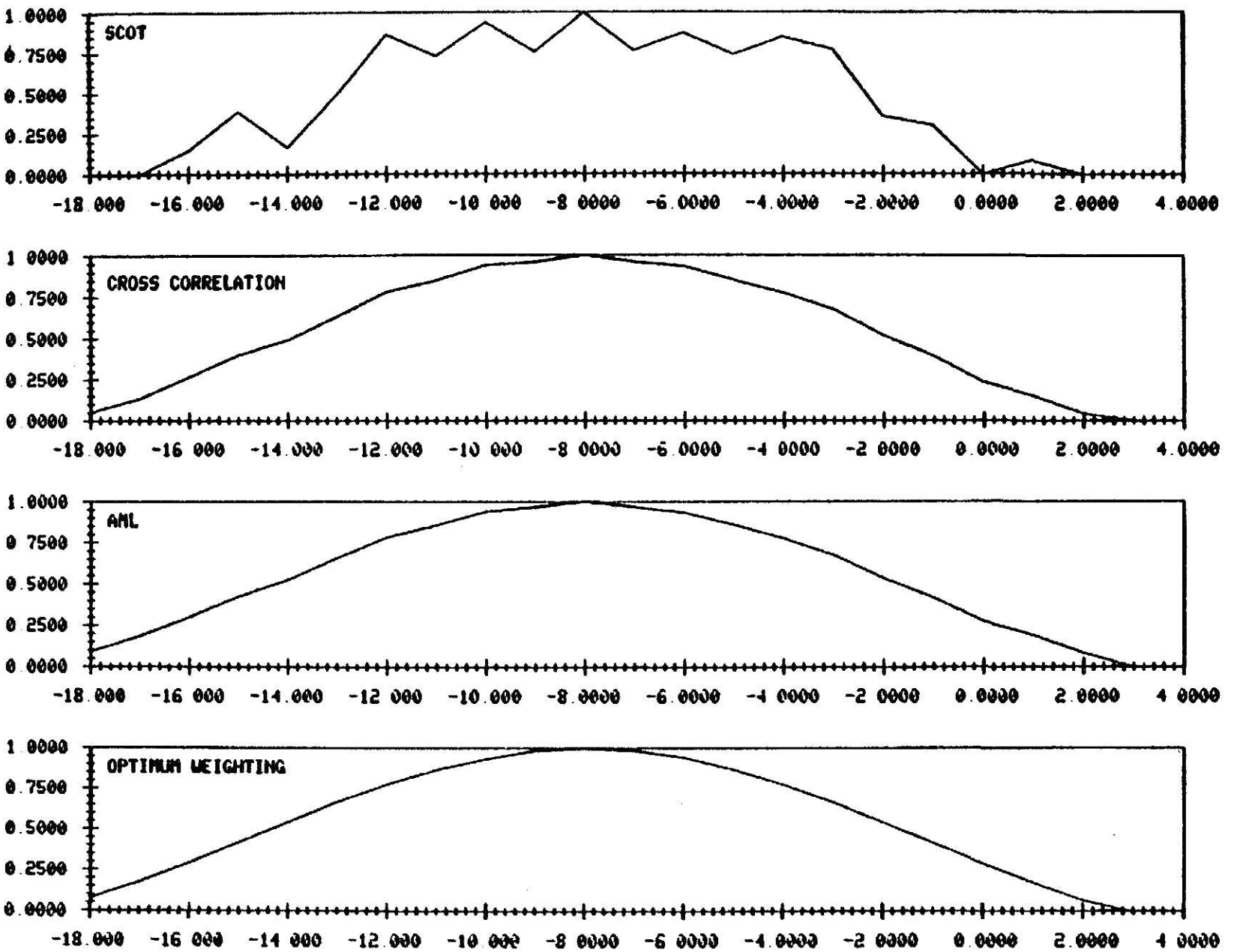

LOW-PASSED CASE - D21--8T - TRIAL 8

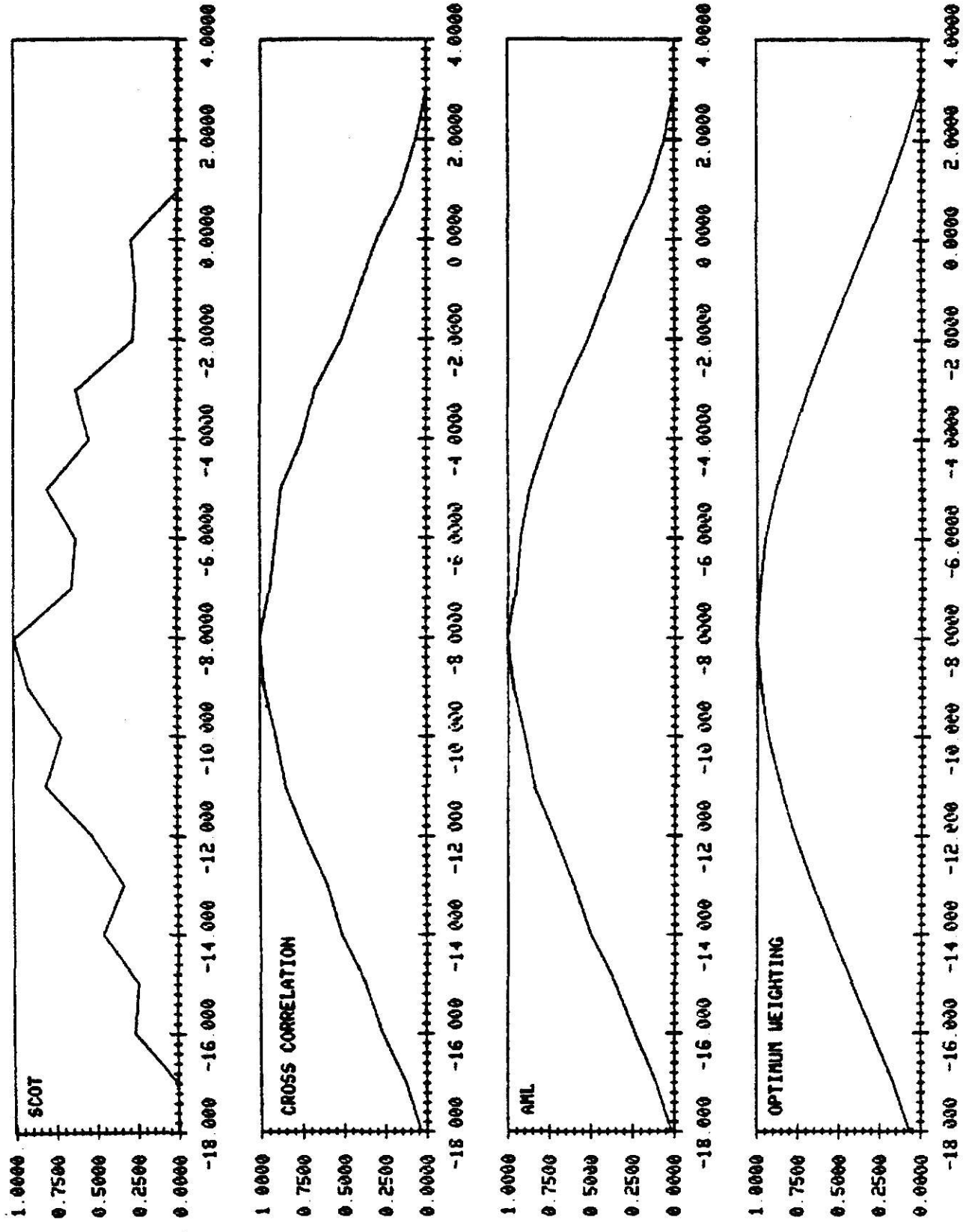

LOW-PASSED CASE - B21=-8T - TRIAL 16

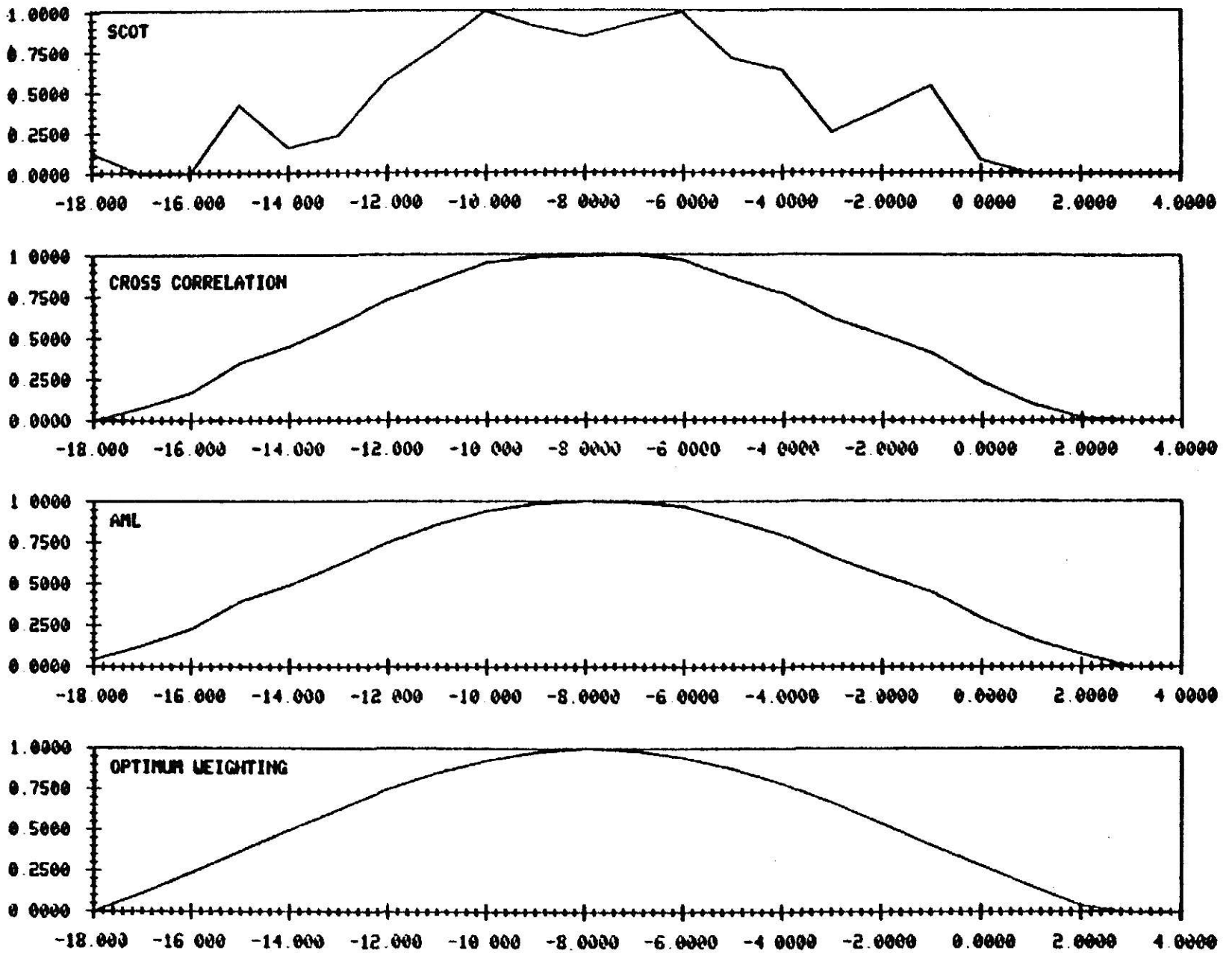

LOW-PASSED CASE - D21--8T - TRIAL 24

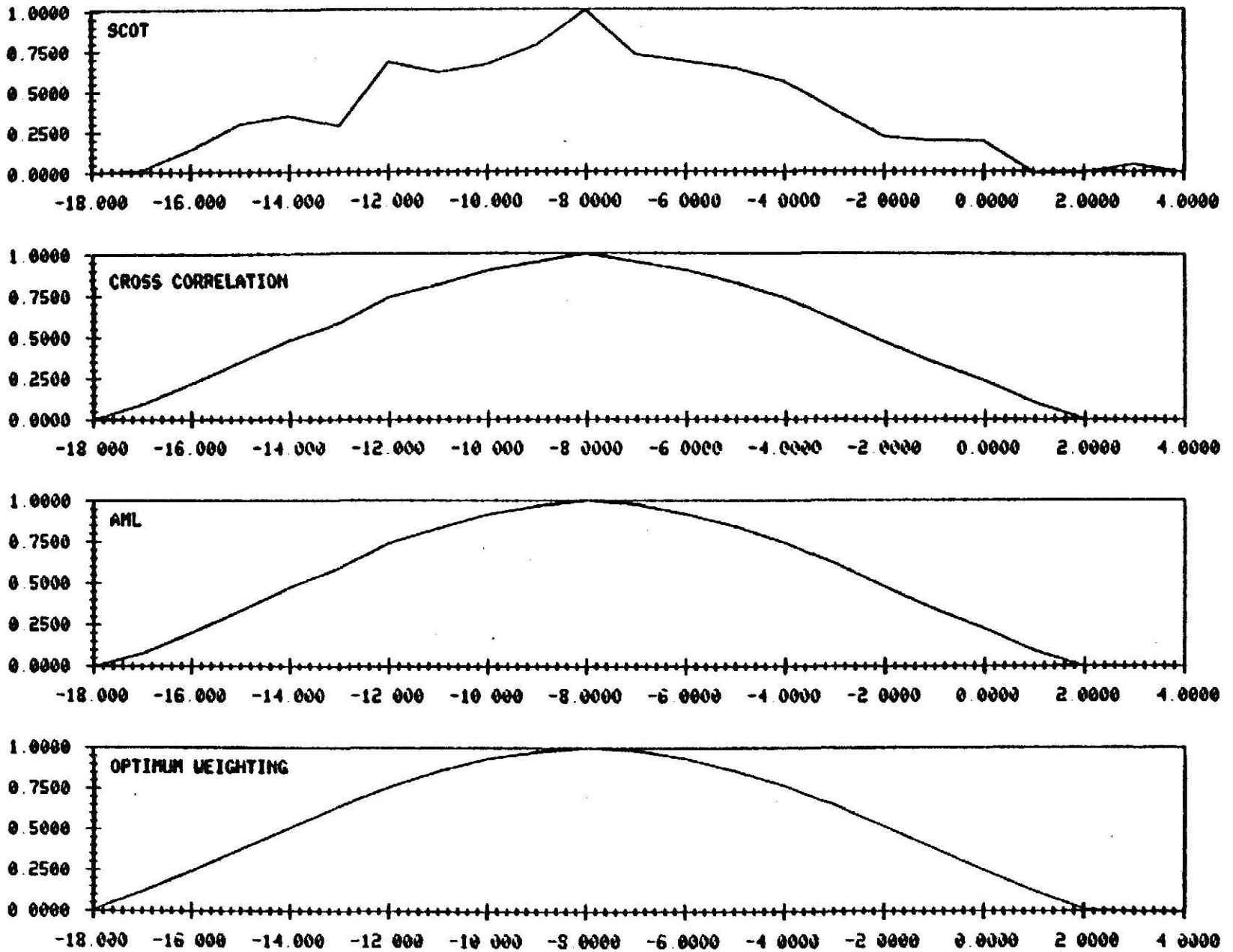

LOW-PASSED CASE - D21--8T - TRIAL 32

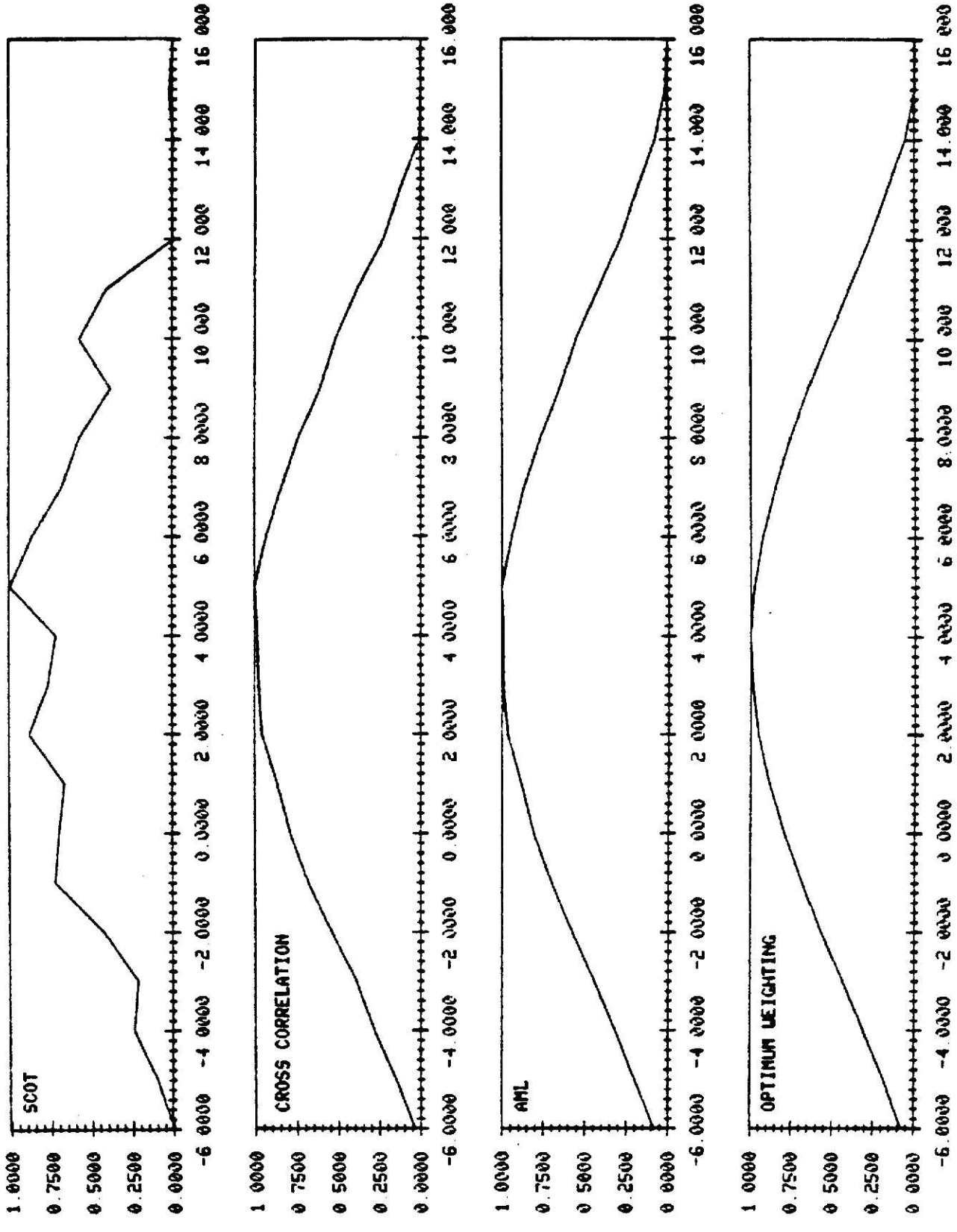

LOW-PASSED CASE - D32-1T - TRIAL 1

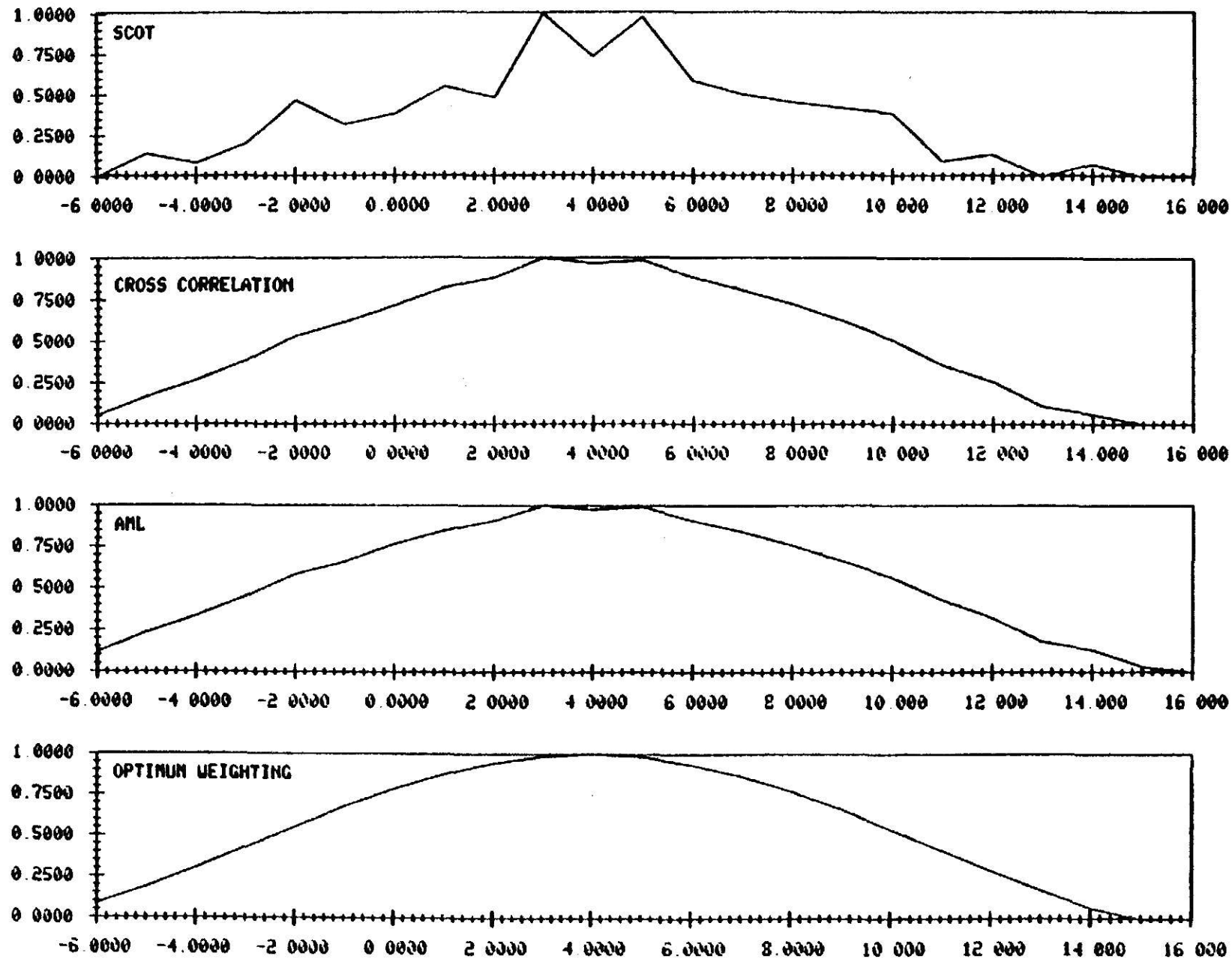

LOW-PASSED CASE - D32-4T - TRIAL 8

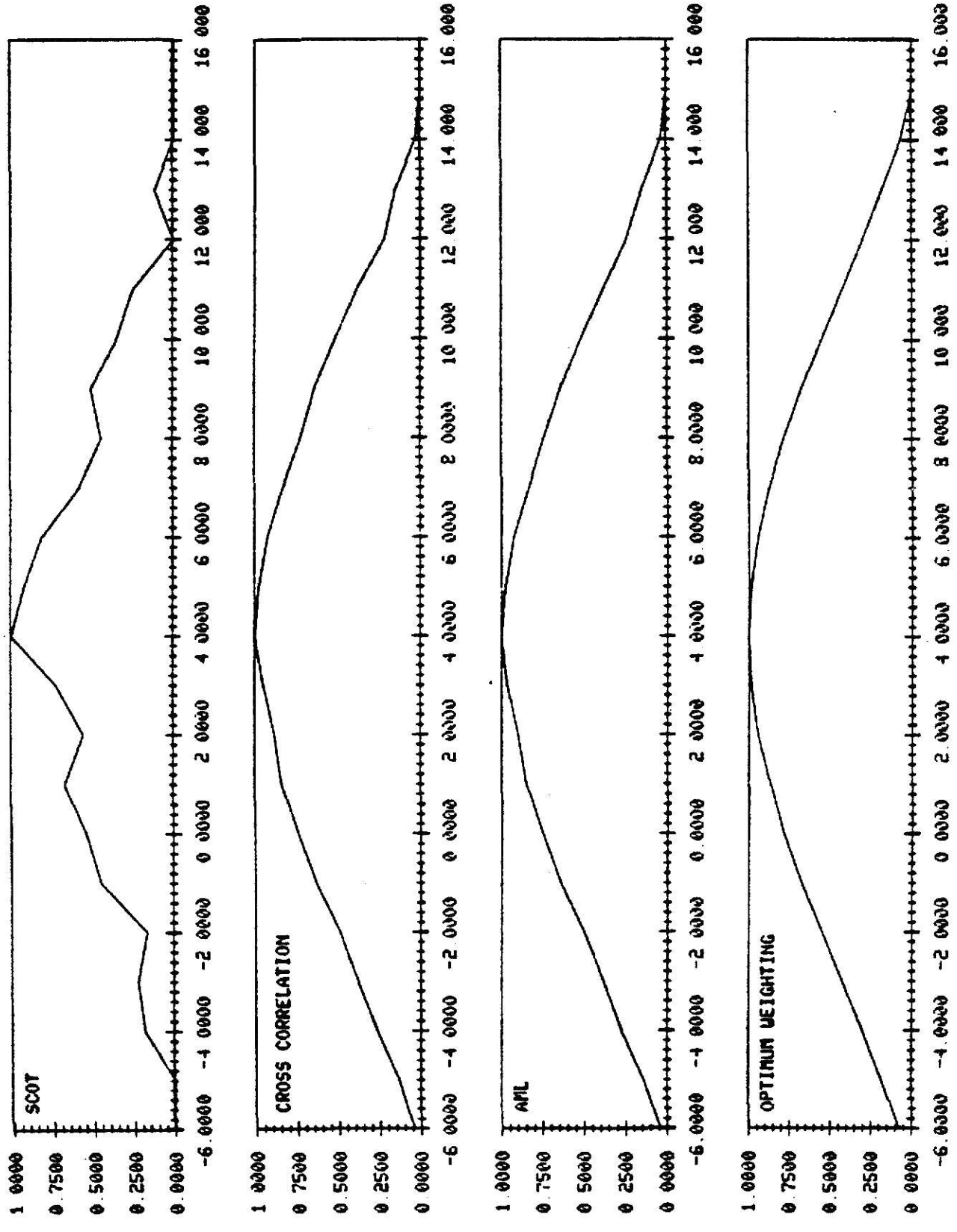

LOW-PASSED CASE - D32-4T - TRIAL 16

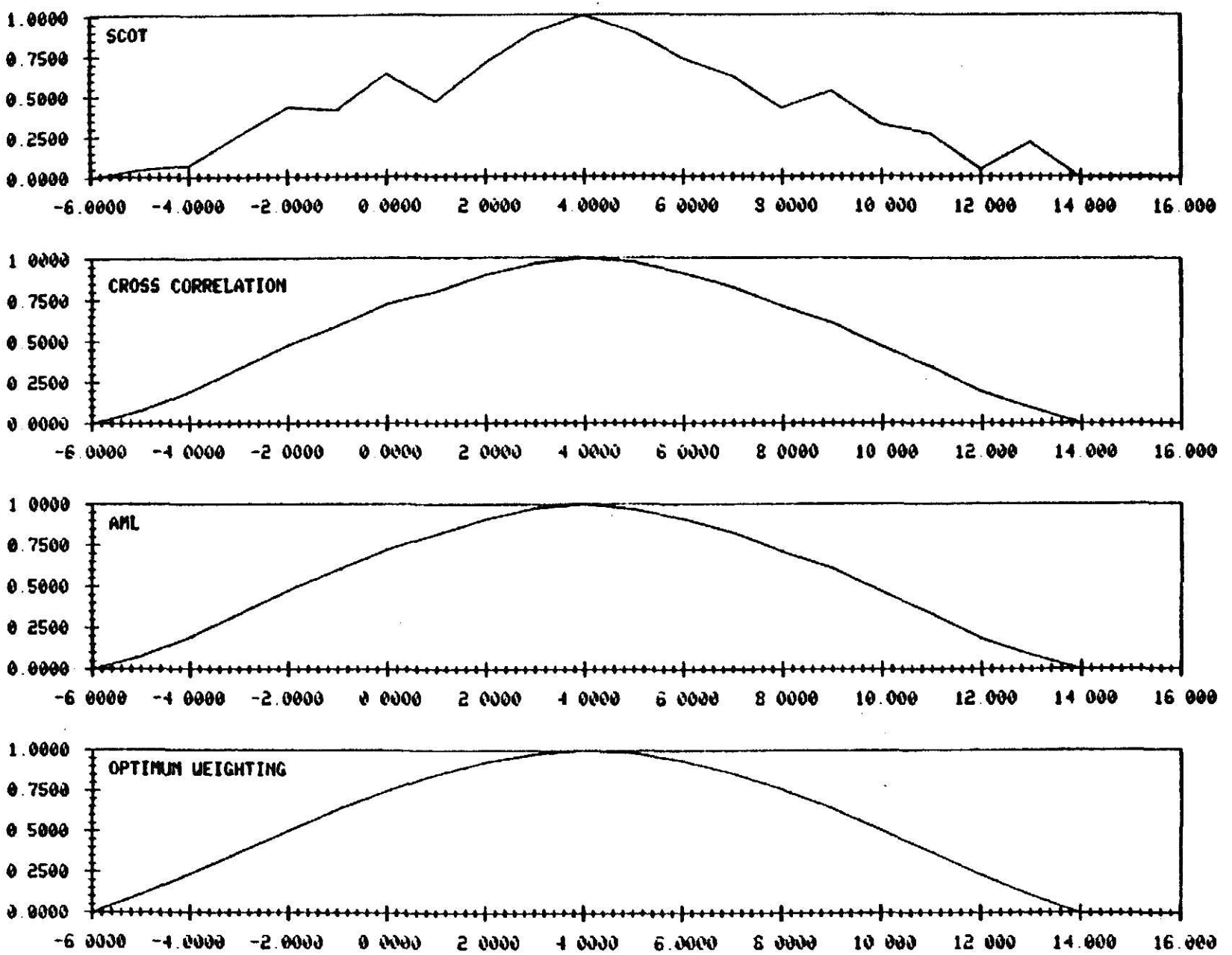

LOW-PASSED CASE - D32-4T - TRIAL 24

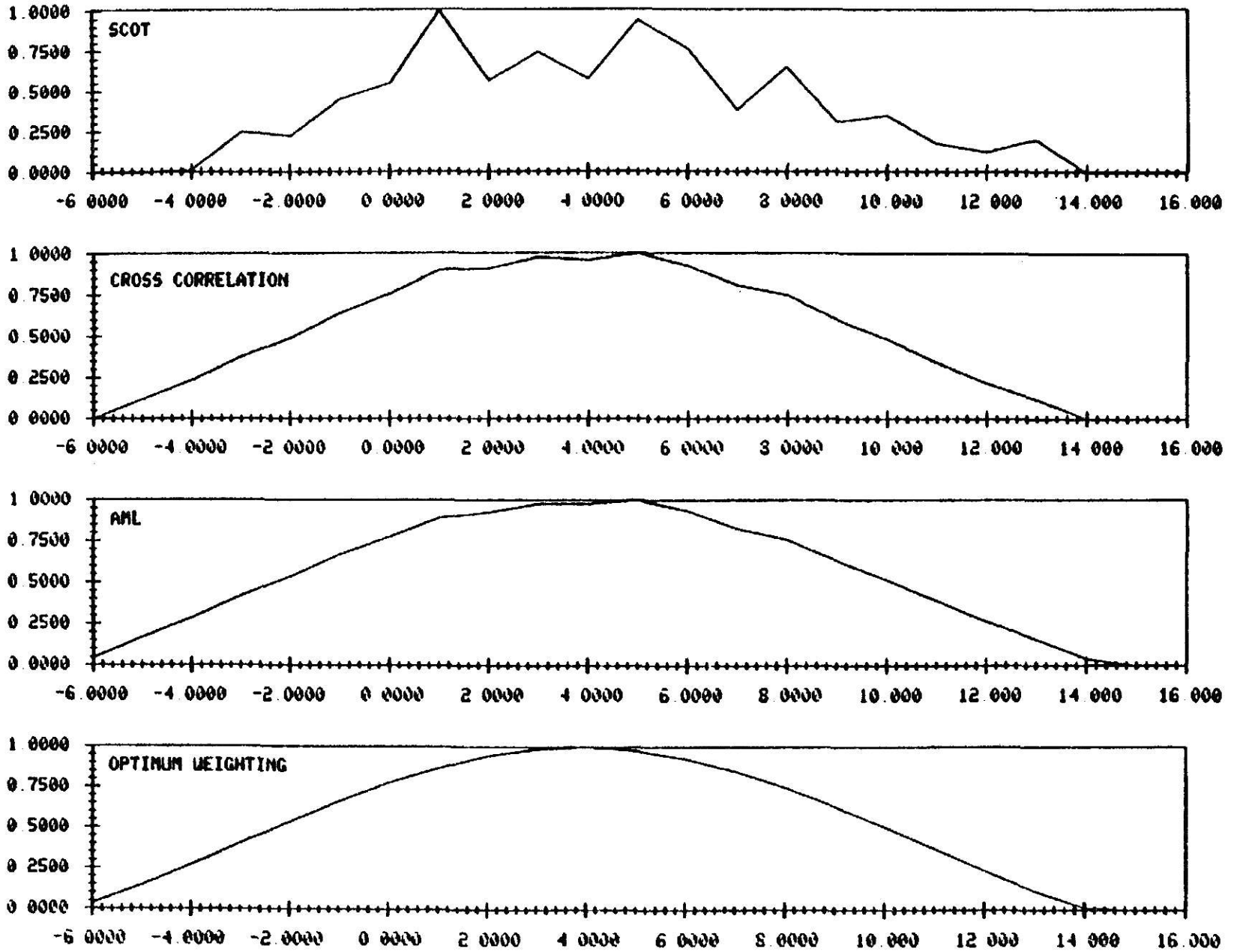

LOW-PASSED CASE - D32-4T - TRIAL 32

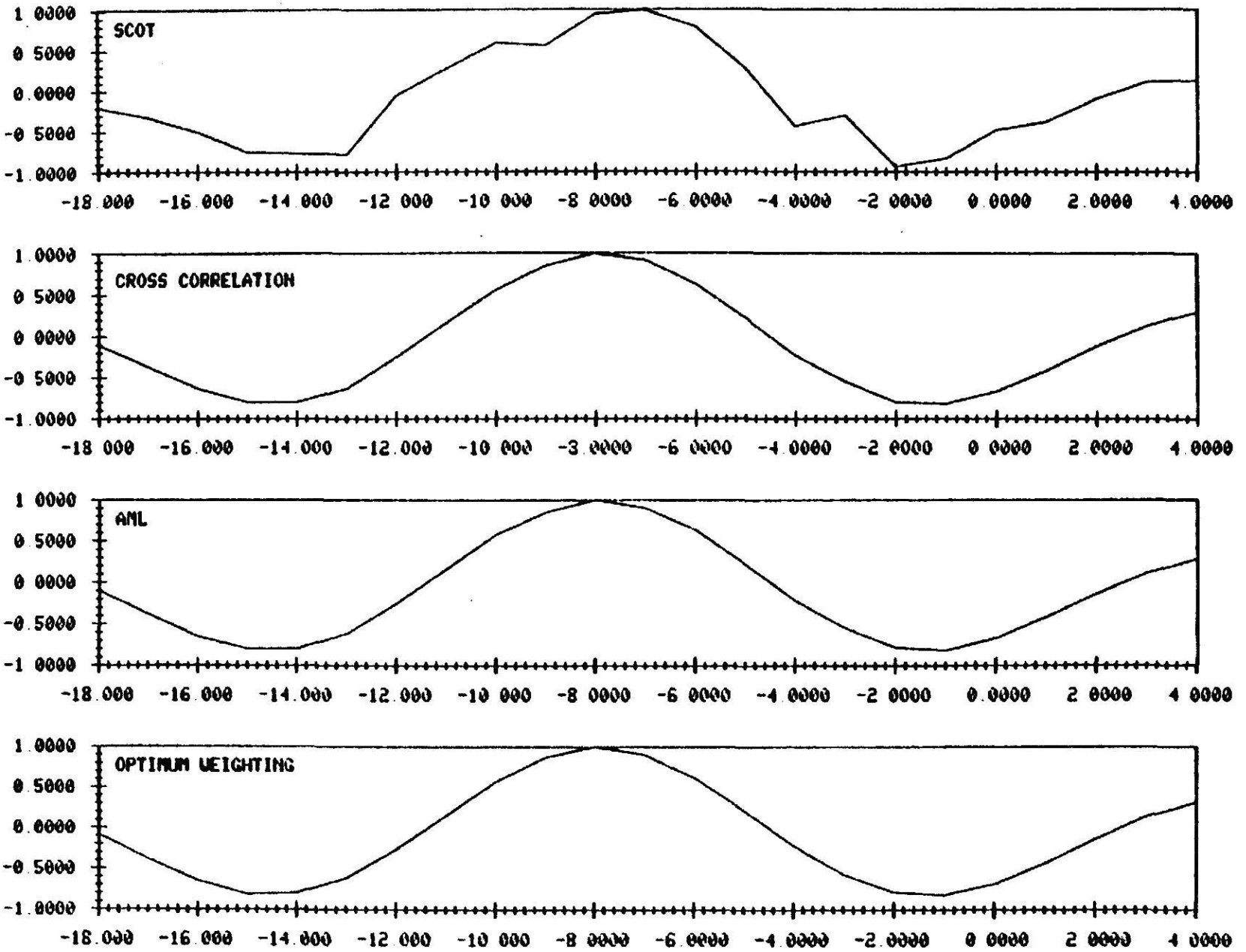

BANDPASSED CASE - D21--8T - TRIAL 1

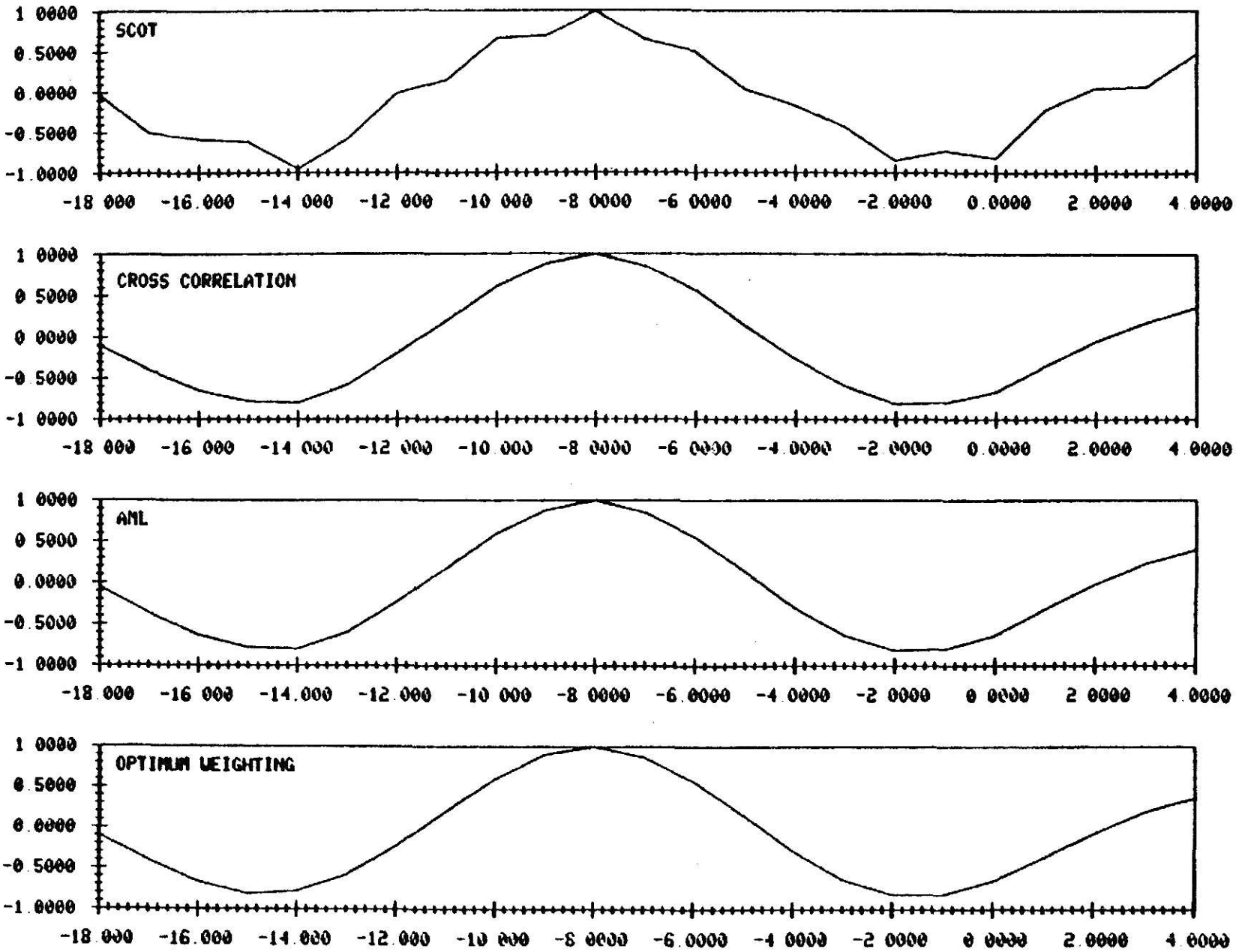

BANDPASSED CASE - D21--8T - TRIAL 8

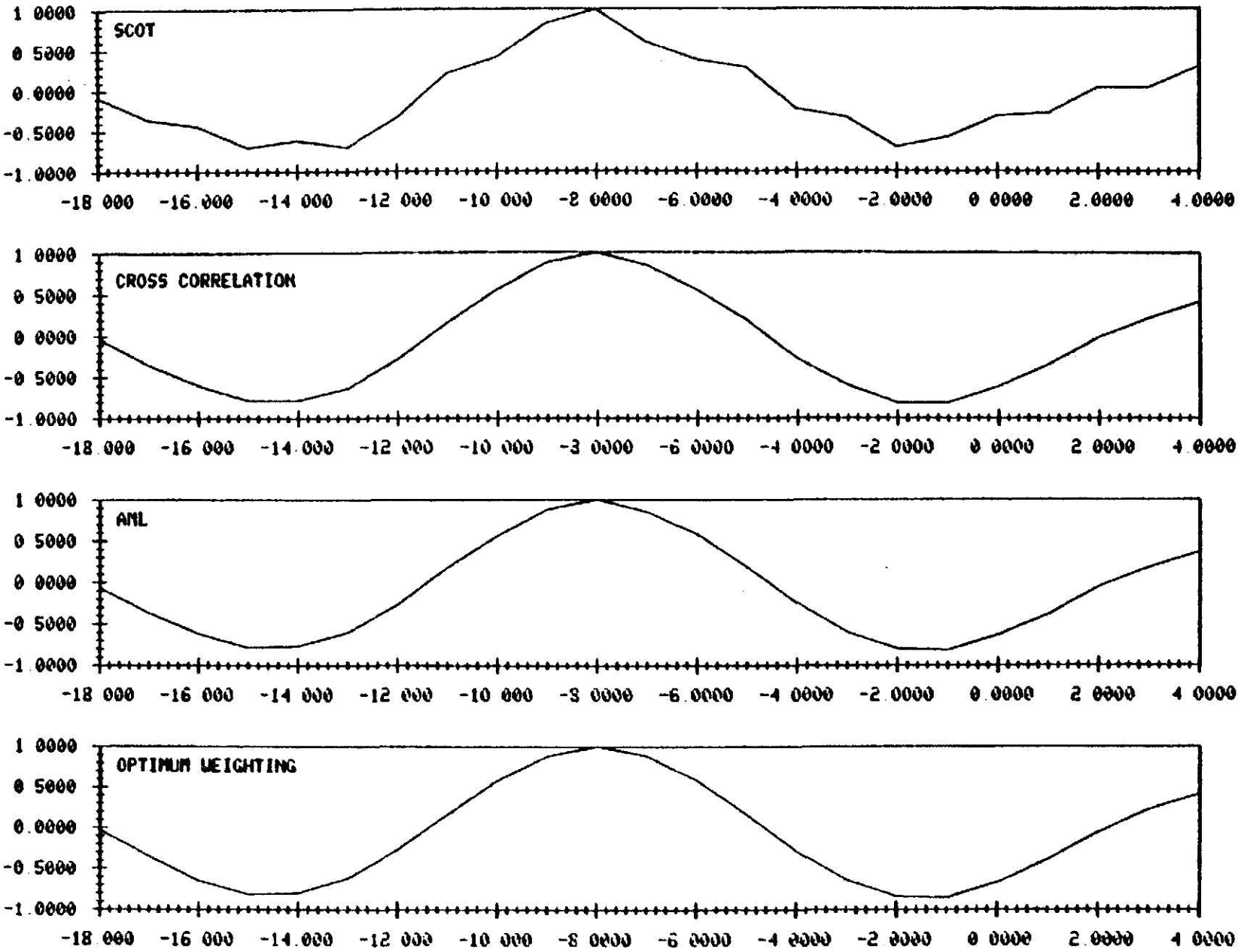

BANDPASSED CASE - D21--8T - TRIAL 16

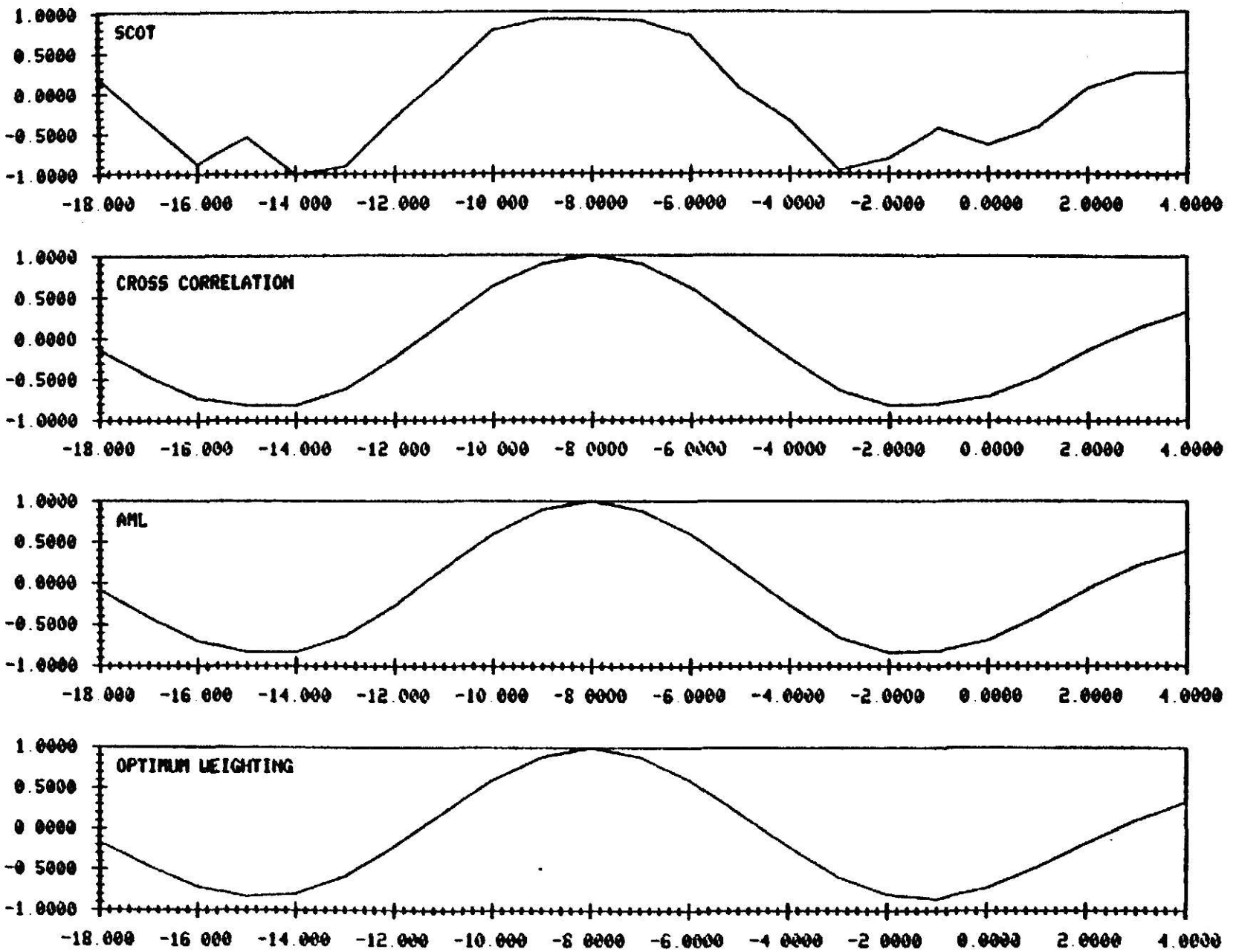

BANDPASSED CASE - D21--8T - TRIAL 24

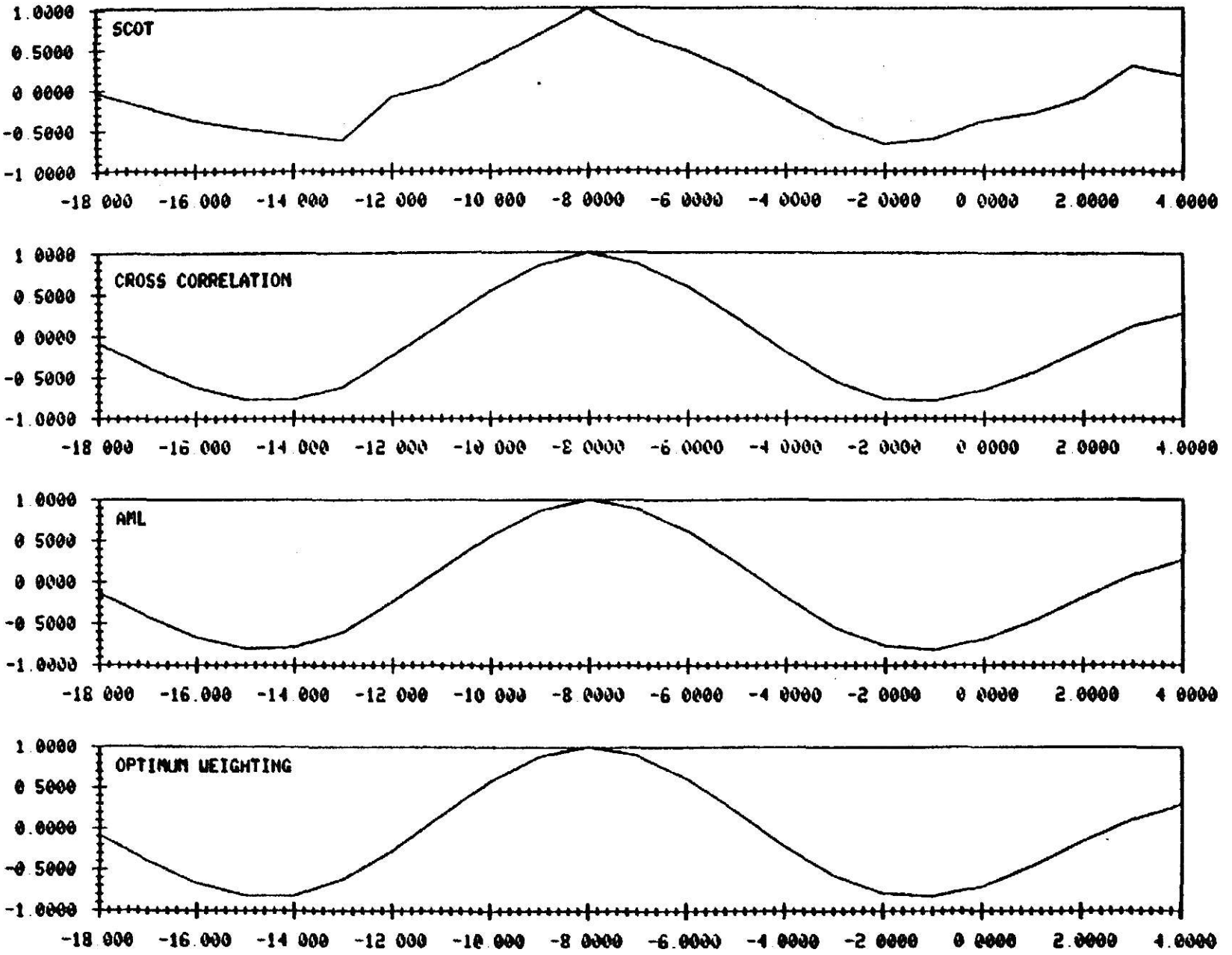

BANDPASSED CASE - D21--8T - TRIAL 32

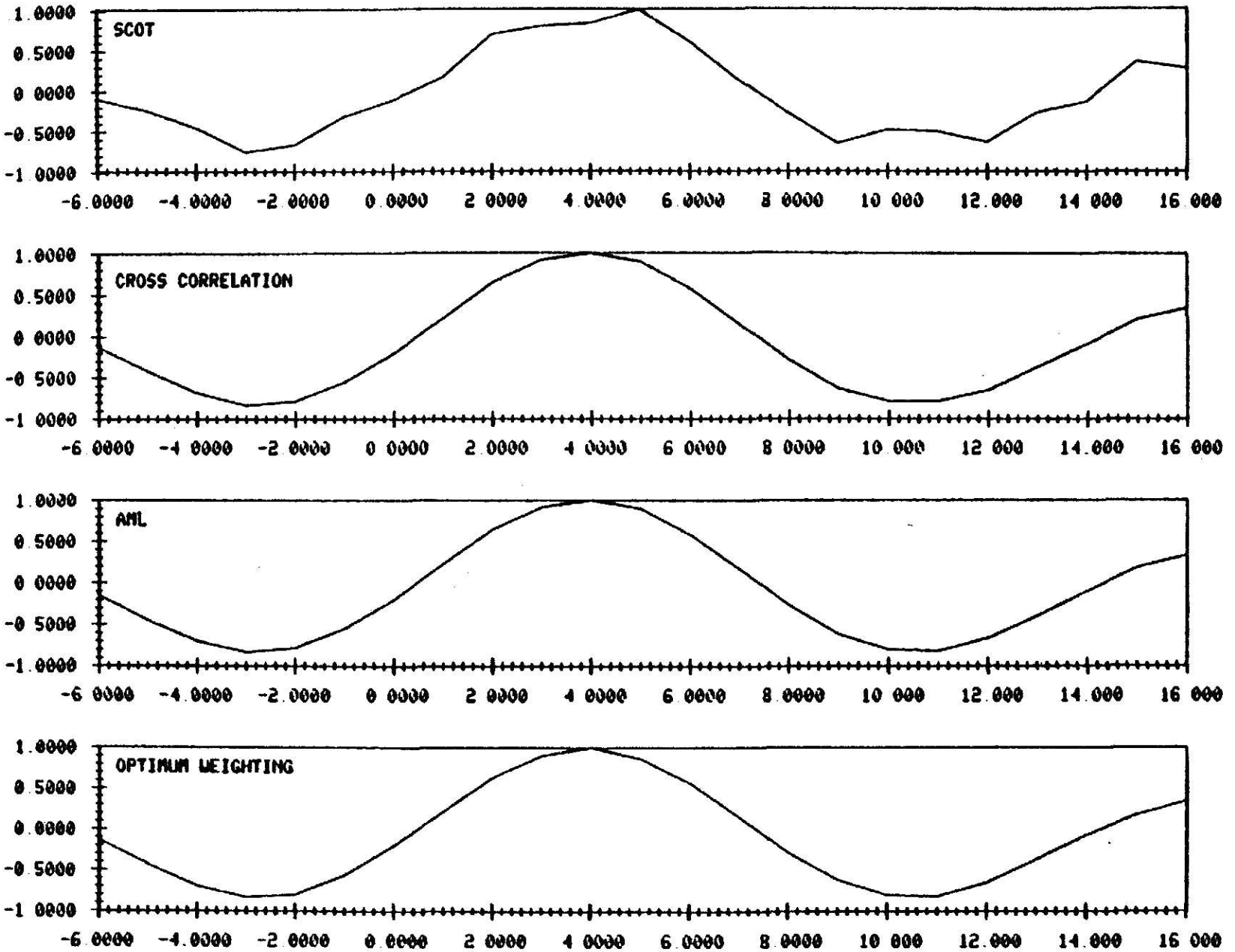

BANDPASSED CASE - D32-4T - TRIAL 1

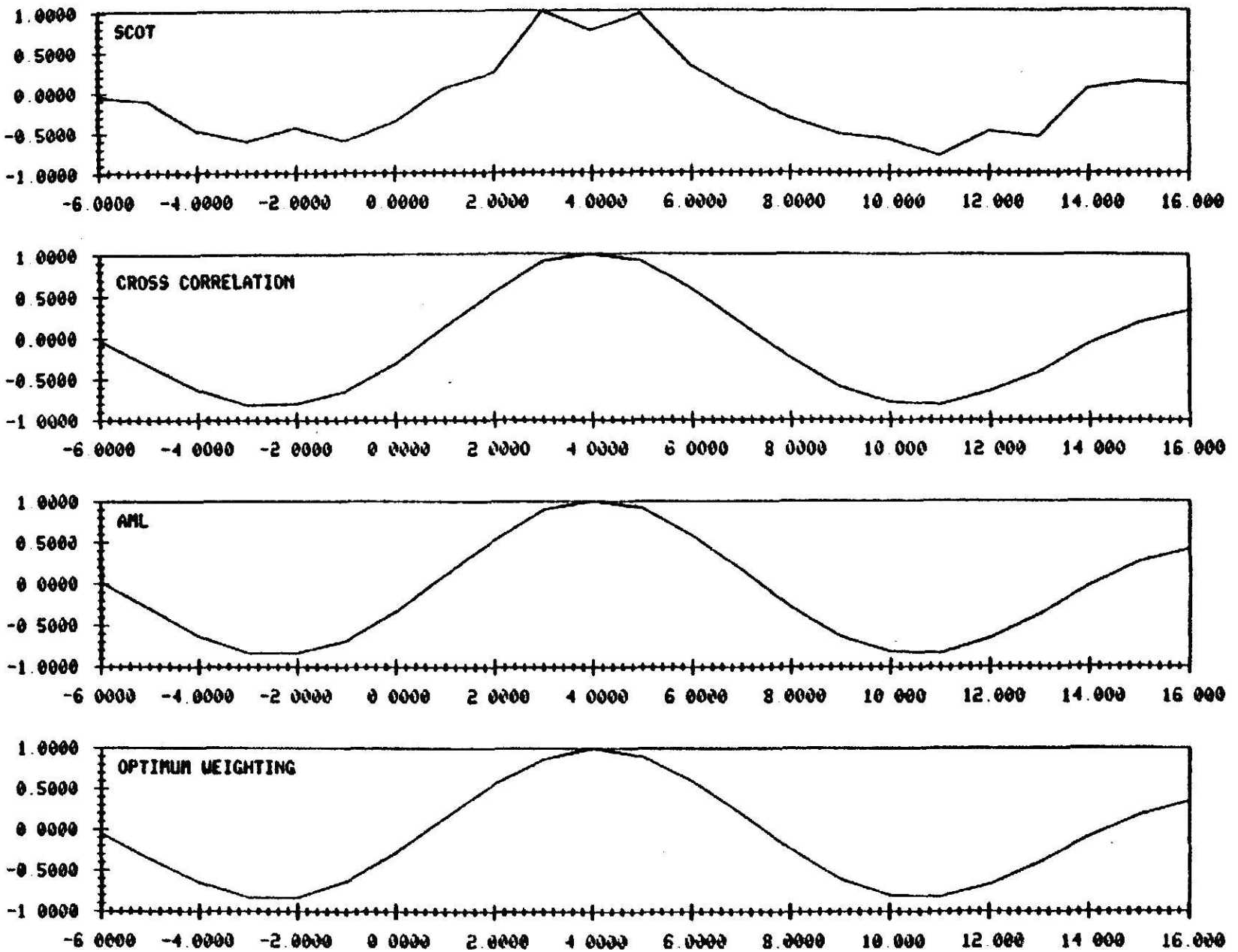

BANDPASSED CASE - D32-4T - TRIAL 8

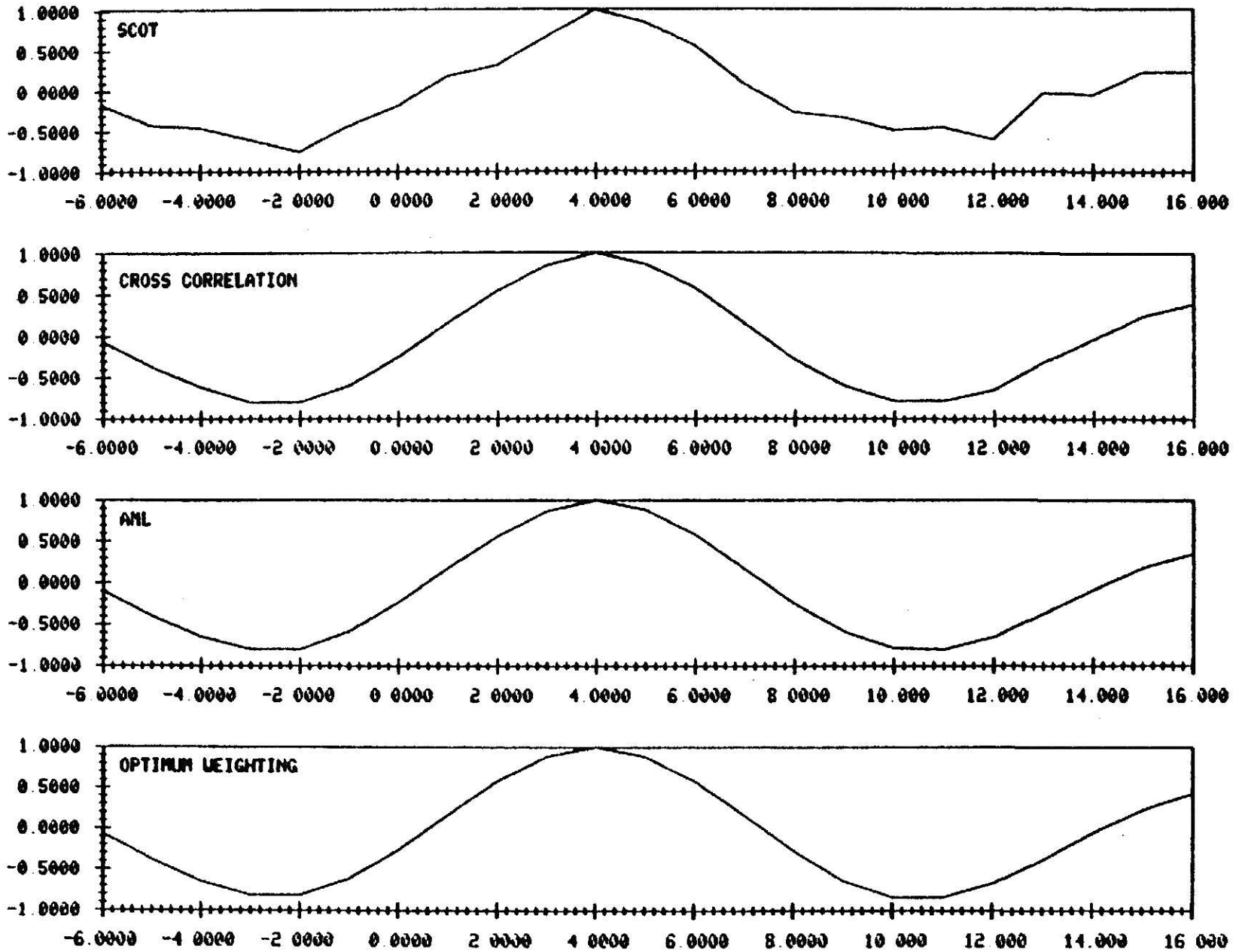

BANDPASSED CASE - D32-4T - TRIAL 16

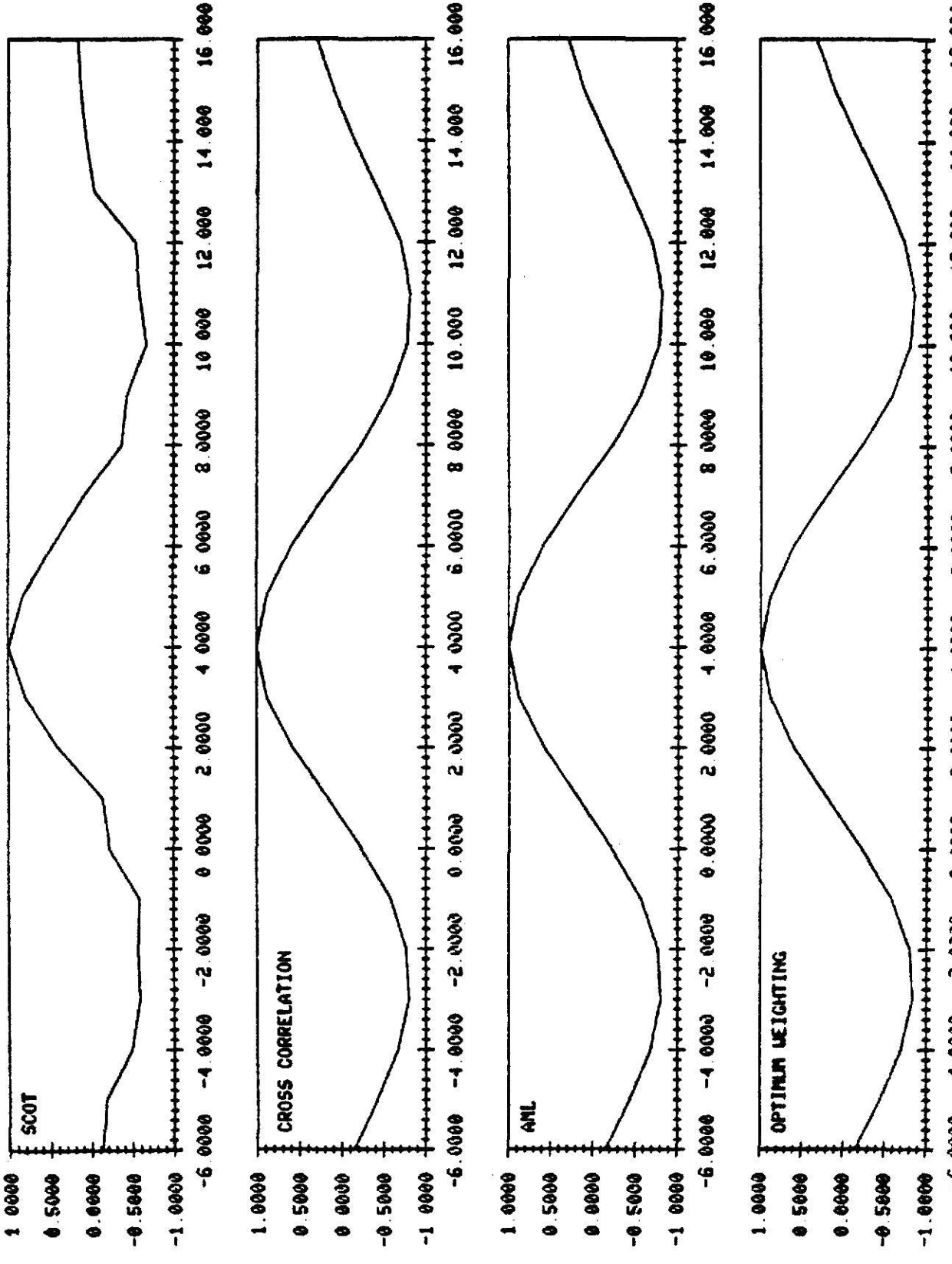

BANDPASSED CASE - D32-4T - TRIAL 24

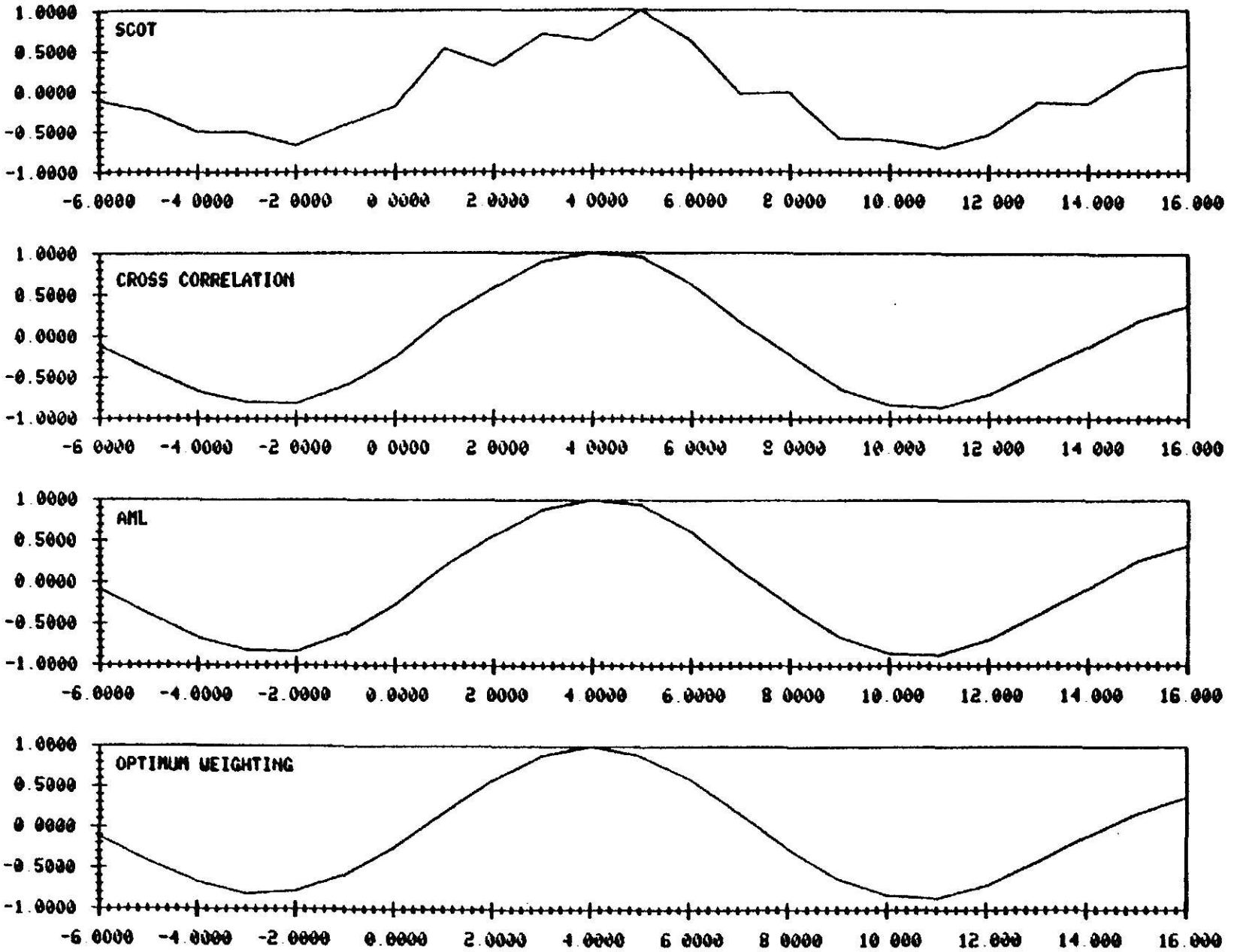

BANDPASSED CASE - D32-4T - TRIAL 32

PERFORMANCE EVALUATION OF TECHNIQUES FOR TIME DELAY ESTIMATION

by

KENT N. SCARBROUGH

B.S., Kansas State University, 1976

AN ABSTRACT OF A MASTER'S REPORT

submitted in partial fulfillment of the

requirements for the degree

MASTER OF SCIENCE

Department of Electrical Engineering

KANSAS STATE UNIVERSITY

Manhattan, Kansas

1980

ABSTRACT

The main objective of this work is to evaluate the performance of the SCOT (smoothed coherence transform) algorithm and an AML (approximate maximum likelihood) estimator, as compared to the basic cross correlation method for time delay estimation. To this end, a digital simulation is employed. The particular case considered is that of a band-limited random signal which is corrupted by white noise and received at three sensors. Using the resulting time delay estimates, estimates of the range of the source are computed. The variances of the time delay estimates and the range estimates are then compared with the corresponding theoretical values.